The role of tonic glycinergic conductance in cerebellar granule cell signalling and the effect of gain-of-function mutation

Catherine McLaughlin[1] (iD), John Clements[2], Ana-Maria Oprişoreanu[3] and Sergiy Sylantyev[4] (iD)

[1] *Gene Therapy Group, The Roslin Institute, University of Edinburgh, Easter Bush, Midlothian, EH25 9RG, UK*
[2] *The John Curtin School of Medical Research, Australian National University, 131 Garran Road, Canberra, ACT 2601, Australia*
[3] *Center for Discovery Brain Sciences, University of Edinburgh, 49 Little France Crescent, Edinburgh, EH16 4SB, UK*
[4] *Center for Clinical Brain Sciences, University of Edinburgh, 49 Little France Crescent, Edinburgh, EH16 4SB, UK*

Edited by: Ole Paulsen & Michisuke Yuzaki

The Journal of Physiology

Key points

- A T258F mutation of the glycine receptor increases the receptor affinity to endogenous agonists, modifies single-channel conductance and shapes response decay kinetics.
- Glycine receptors of cerebellar granule cells play their functional role not continuously, but when the granule cell layer starts receiving a high amount of excitatory inputs.
- Despite their relative scarcity, tonically active glycine receptors of cerebellar granule cells make a significant impact on action potential generation and inter-neuronal crosstalk, and modulate synaptic plasticity in neural networks; extracellular glycine increases probability of postsynaptic response occurrence acting at NMDA receptors and decreases this probability acting at glycine receptors.
- Tonic conductance through glycine receptors of cerebellar granule cells is a yet undiscovered element of the biphasic mechanism that regulates processing of sensory inputs in the cerebellum.
- A T258F point mutation disrupts this biphasic mechanism, thus illustrating the possible role of the gain-of-function mutations of the glycine receptor in development of neural pathologies.

Abstract Functional glycine receptors (GlyRs) have been repeatedly detected in cerebellar granule cells (CGCs), where they deliver exclusively tonic inhibitory signals. The functional role of this signalling, however, remains unclear. Apart from that, there is accumulating evidence of the important role of GlyRs in cerebellar structures in development of neural pathologies such as hyperekplexia, which can be triggered by GlyR gain-of-function mutations. In this research we initially tested functional properties of GlyRs, carrying the yet understudied T258F gain-of-function mutation, and found that this mutation makes significant modifications in GlyR response to endogenous agonists. Next, we clarified the role of tonic GlyR conductance in

Following a BSc in genetics and cell biology and Masters in genetic engineering and novel therapeutics, **Catherine McLaughlin** gained a research position in Seth Grant's laboratory focused on genome editing with primary and differentiated cell screening to develop improved cell assay platforms. Now based in The Roslin Institute, as part of the Gene Therapy Group, her research is concentrated on emerging genetic therapies and their optimization for human clinical trials.
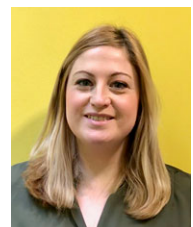
neuronal signalling generated by single CGCs and by neural networks in cell cultures and in living cerebellar tissue of C57Bl-6J mice. We found that GlyRs of CGCs deliver a significant amount of tonic inhibition not continuously, but when the cerebellar granule layer starts receiving substantial excitatory input. Under these conditions tonically active GlyRs become a part of neural signalling machinery allowing generation of action potential (AP) bursts of limited length in response to sensory-evoked signals. GlyRs of CGCs support a biphasic modulatory mechanism which enhances AP firing when excitatory input intensity is low, but suppresses it when excitatory input rises to a certain critical level. This enables one of the key functions of the CGC layer: formation of sensory representations and their translation into motor output. Finally, we have demonstrated that the T258F mutation in CGC GlyRs modifies single-cell and neural network signalling, and breaks a biphasic modulation of the AP-generating machinery.

Introduction

Tonic inhibitory signalling is one of the key modulatory mechanisms of neural cell crosstalk and, as a consequence, neural network functioning in the brain (Farrant & Nusser, 2005). This form of signalling is commonly mediated by extrasynaptic receptors with a high affinity to neurotransmitter ejected into the extracellular space due to synaptic spillover (Eulenburg & Gomeza, 2010). Despite active research over past decades, our understanding of tonic inhibitory signalling mechanisms is still far from excellent. To date, the vast majority of studies examining the mechanisms of tonic inhibition have concentrated on that mediated by GABA$_A$ receptors (GABA$_A$Rs) (Mtchedlishvili & Kapur, 2006; Mann & Mody, 2009; Clarkson *et al.* 2010). In contrast, much less attention has been paid to glycine receptors (GlyRs), which are also expressed extrasynaptically and can generate lasting inhibitory tone (Xu & Gong, 2010; Salling & Harrison, 2014).

Cerebellar granule cells (CGCs) make a favourable model system to address the role of inhibitory conductance in information processing. CGCs are electrically compact, which allows high-resolution patch-clamp and makes them sensitive to small fluctuations of electrical conductance (Virginio & Cherubini, 1997) and undergo strong inhibition (Rossi *et al.* 2003; Chadderton *et al.* 2004); they form a continuous input layer which shapes information flow through the cerebellar cortex (Hamann *et al.* 2002; Chadderton *et al.* 2004).

Concentration values for glycine (Gly) in the extracellular space of cerebellar tissue display quite a noticeable difference when reported by different research groups: $8.6 \pm 2 \mu M$ (Tossman *et al.* 1986), $18 \pm 9 \mu M$ (Matsui *et al.* 1995), $27 \pm 12 \mu M$ (Hashimoto *et al.* 1995). Despite these differences, the cerebellum is a part of the brain with one of the highest extracellular concentrations of Gly (Tossman *et al.* 1986), thus suggesting an important role of glycinergic signalling in cerebellar function.

In the cerebellum, the highest density of GlyRs at cell surfaces was demonstrated for Purkinje cells and interneurons of the molecular layer, with a low, but detectable, immune signal in all other areas (van den Pol & Gorcs, 1988; Sassoè-Pognetto *et al.* 2000). Using molecular biology methods, GlyRs have been also found in CGCs, being localized at cell somata rather than within synaptic densities (van den Pol & Gorcs, 1988). Further electrophysiological studies have revealed fully functional GlyRs in membrane patches excised from CGC somata (Kaneda *et al.* 1995; Virginio & Cherubini, 1997), but no GlyR-mediated signalling in CGC synapses (Kaneda *et al.* 1995). These data imply that the GlyRs of CGCs are exclusively (or at least to a major extent) localized to the extrasynaptic cell surface, thus enabling research into tonic GlyR-mediated inhibition without 'contaminating' signalling from synaptic glycinergic inhibitory transmission.

Inhibitory GlyRs are pentameric Cl$^-$ channels; functional GlyR can be homomeric, i.e. consist of five α subunits ($\alpha1$–$\alpha4$ subtypes), or heteromeric with a $3\alpha + 2\beta$ composition (Langosch *et al.* 1988). The latter composition type is most typical for acute neural tissue. The T258F point mutation in the $\alpha1$ subunit is a gain-of-function mutation which was shown to increase affinity to glycine (Gly) in both homomeric and heteromeric GlyRs (Steinbach *et al.* 2000; Shan *et al.* 2001). Hence, T258F $\alpha1$-containing GlyRs of various subunit compositions facilitate the study of tonic inhibitory conductance, as they can be activated by relatively low concentrations of endogenous ligands characteristic of the extrasynaptic space. However, following initial interest, studies of the T258F GlyR have been paused for more than 15 years, and thus its pharmacology in respect to ligands other than Gly, its impact on inhibitory response kinetics,

not to mention its functional role in inter-neuronal signalling remain unknown.

Hyperekplexia, or startle disease, is a neuromotor disorder caused by deficits in glycinergic brain signalling and, at least in some cases, associated with cerebellar vermis (Leaton & Supple, 1986; Lopiano *et al.* 1990). Gain-of-function mutations of the GlyR $\alpha 1$ subunit were repeatedly shown to cause hyperekplexia (Chung *et al.* 2010; Bode *et al.* 2013) via the ablation of $\alpha 1 \beta$ glycinergic synapses (Zhang *et al.* 2016). This is, however, unlikely the case for the cerebellar effects associated with CGCs due to the absence (or extreme scarcity) of glycinergic synaptic connections at these cells. Thus the dissection of the effects of GlyRs carrying gain-of-function mutation in CGCs may provide a key to cellular and molecular hyperekplexia mechanisms which are currently not the focus of neuroscience research.

Apart from Gly (Billups & Attwell, 2003), another endogenous GlyR ligand released in cerebellum upon depolarization is β-alanine (Ala) (Saransaari & Oja, 1993; Koga *et al.* 2002). Despite being much less potent than Gly, when acting at the GlyR (Pan & Slaughter, 1995), endogenous Ala has been shown to generate tonic GlyR-mediated current in living neural tissue (Mori *et al.* 2002).

Therefore, in this study we dissect the role in neuronal signalling and functional properties of the T258F GlyR in comparison with the wild-type (WT) receptor after activation by Gly and Ala. We set out to go from volatility of single-channel electrical conductance to the impact of tonic GlyR-mediated current on cerebellar neural network functioning, connecting these points via the modulation of inhibitory response kinetics and the regulation of action potential generation.

Methods

Ethical approval

All experiments on animals were conducted in strict accordance with the UK Animals (Scientific Procedures) Act 1986 Schedule 1 and the Australian National University ethical committee regulations.

HEK cell cultures

Human embryo kidney 293 (HEK-293) cells were grown in 10 cm tissue culture dishes coated with a mixture of rat tail Type I collagen at 0.5 mg/ml and poly-D-lysine at 0.1 mg/ml at 37°C, 5% CO_2, in a saturated water atmosphere, cultivated in minimum essential medium, supplemented with 10% fetal calf serum, 100 IU penicillin, 100 μg/l streptomycin, and passaged twice weekly.

Since expression of the $\alpha 2$ GlyR subunit in CGCs sharply decreases during the first 3 weeks of postnatal development to the level characteristic of the adult organism, whereas expression of $\alpha 1$ and β subunits increases over the same period (Lynch, 2009), we transfected HEK cells and cultured CGCs with $\alpha 1$ subunit DNA to mimic a receptor composition characteristic for 25- to 30-day-old animals, which were used as a source of acute cerebellar tissue.

HEK-293 cells were transfected by a calcium phosphate–DNA coprecipitation protocol (Chen & Okayama, 1987) with cDNA coding for the $\alpha 1$ glycine receptor subunit (T258F or WT) and β subunit (WT) and for green fluorescent protein (GFP) as a marker. When co-transfecting the GlyR $\alpha 1$ and β subunits, their respective cDNAs were combined in a ratio of 1:10 (Pribilla *et al.* 1992). Recordings were carried out 24–72 h after transfection. The perfusion solution contained (in mM): 140 NaCl, 4 KCl, 2 $CaCl_2$, 2 $MgCl_2$, 10 HEPES, 10 glucose; pH was adjusted to 7.4 with NaOH, osmolarity 300–310 mOsm. Recording pipettes were made from borosilicate glass capillaries, 1.5 mm OD, 0.86 mm ID. Pipettes used for whole-cell recordings had resistances of 2–3 MΩ, for patch recordings 4–5 MΩ. Both pipettes for patch- and whole-cell recordings contained (in mM): 145 CsCl, 2 $CaCl_2$, 2 $MgCl_2$, 10 HEPES, 10 EGTA, with the pH adjusted to 7.4 with CsOH and osmolarity adjusted to 300–310 mOsm. Drug application was performed using an eight-channel set of U-tubes, and ligands were dissolved in perfusion solution. The flow pipes had an individual tip diameter of approximately 40 μm and were arranged in a square pattern. For the rapid solution application experiment we adapted a Rapid Application and Solution Exchange (RASE) protocol (Sylantyev & Rusakov, 2013) allowing application of a series of different solutions at the same patch with up to 150–200 μs time resolution. Briefly, patches were exposed to the solution flow from a θ-glass pipette mounted on a piezo-actuator, with up to three different solutions exchanged in each application pipette channel; solution application on the patch pipette tip was performed by switches of piezo-actuator driven by a DSA-2 constant-voltage stimulus isolator (Digitimer Ltd, Welwyn Garden City, UK). Experiments were performed at 33–35°C with a holding potential of –60 or –70 mV. Data acquisition and online analysis were performed with AxoGraph 4.0 (AxoGraph Ltd, Canberra ACT, Australia) and pClamp/Clampfit 10x software (Molecular Devices LLC, San Jose, CA, USA). Analysis of current transients activated by +5 mV voltage steps in voltage-clamp mode gave 11.17 ± 0.2 pS as a value of HEK cell membrane capacitance ($n = 217$), which reproduces earlier reports (Avila *et al.* 2004; Fischmeister & Hartzell, 2005).

Cerebellar acute slices

C57Bl-6J mice were bred in the institutional animal house, grown on a Rat and Mouse Breeding Diet (Special

Diet Services, Witham, UK) and water *ad libitum*, and maintained at a 12–12 h light–dark cycle. Animals were sacrificed for slices in the first half of the light period of the light–dark cycle. To kill animals, we used an overdose of isoflurane according to the UK Animals (Scientific Procedures) Act 1986. After decapitation with a guillotine, brains were rapidly removed and dissected, and cerebellums were sliced.

Parasagittal slices of 250 μm were cut from the cerebellar vermis of 25- to 30-day-old mice with a Leica VT1200S vibraing blade microtome and incubated for 1 h in a solution containing (in mM): 124 NaCl, 3 KCl, 1 CaCl$_2$, 3 MgCl$_2$, 26 NaHCO$_3$, 1.25 NaH$_2$PO$_4$, 10 D-glucose, and bubbled with 95% O$_2$–5% CO$_2$, pH 7.4. After incubation slices were transferred to a recording chamber continuously superfused with an external solution. The external solution composition differed from the incubation solution in containing 2 mM CaCl$_2$ and 2 mM MgCl$_2$. GlyR-delivered conductance was isolated with a ligand cocktail containing 50 μM (2R)-amino-5-phosphonovaleric acid (APV), 20 μM 2, 3-dihydroxy-6-nitro-7-sulfamoyl-benzo[f]quinoxaline-2, 3-dione (NBQX), 50 nM CGP-55845, 200 μM (S)-α-methyl-4-carboxyphenylglycine (S-MCPG), 10 μM MDL-72222, and 1 mM pentylenetetrazole (PTZ) as GABA$_A$-receptor antagonist which has no or low impact on GlyR effects (Corda *et al.* 1991; Blednov *et al.* 2012), which is not the case for other commonly used antagonists of GABA$_A$-receptor (Wang & Slaughter, 2005).

The mossy fibre–granule cell pathway morphology is identical for the whole cerebellum; thus any part of cerebellar granule cell layer with adjacent white matter can be used as a representative experimental object. However, to preserve the pathway intact in biplanar slice, vermis rather than cerebellar hemispheres should be used: otherwise, due to bends of lobules in three dimensions, a biplanar slice breaks into small separate pieces (Garthwaite & Batchelor, 1996). Therefore, in our preparation we used slices of cerebellar vermis, where high-frequency stimulation was delivered to mossy fibre axons by a DSA-2 stimulus isolator via a bipolar tungsten electrode placed in the cerebellar white matter near the gyrus crest to stimulate mossy fibres entering the granule cells layer (Garthwaite & Batchelor, 1996). To stimulate a single mossy fibre, we used a θ-glass electrode pulled to ~5 μm tip diameter, filled with perfusion solution, with wires in both channels connected to the stimulus isolator.

In all experiments on CGCs (in acute tissue or in culture) the intracellular pipette solution for voltage-clamp recordings contained (mM): 117.5 caesium gluconate, 17.5 CsCl, 10 KOH-HEPES, 10 BAPTA, 8 NaCl, 5 QX-314, 2 Mg-ATP, 0.3 GTP; for current-clamp recordings: 126 potassium gluconate, 4 NaCl, 5 HEPES, 15 glucose, 1 MgSO4.7H$_2$O, 2 BAPTA, 3 Mg-ATP; pH 7.2, 295 mOsm in both cases; pipette resistance was 7–9 MΩ; recordings were performed at 33–35°C using a Multiclamp-700B amplifier (Molecular Devices LLC) with –60 or –70 mV holding voltage (for voltage-clamp recordings); signals were pre-filtered and digitized at 10 kHz.

Cultured granule cells

Primary cultures of cerebellar granule neurons were prepared from postnatal day 25–27 mice. Animals were sacrificed as described above. The cerebellums were then removed, dissociated with 0.25 mg/ml trypsin, and plated in 35 mm Nunc dishes at a density of 1.5 × 10^4 cells/ml on glass coverslips coated with poly-D-lysine (10 μg/ml). The cells were cultured in basal Eagle's medium supplemented with 10% bovine calf serum, 2 mM glutamine, and 100 μg/ml gentamycin at 37°C in 5% CO$_2$. At day *in vitro* (DIV) 5 the medium was replaced with 5 mM K$^+$ medium supplemented with 5 mg/ml glucose, 0.1 mg/ml transferrin, 0.025 mg/ml insulin, 2 mM glutamine, 20 μg/ml gentamycin and 10 μM cytosine arabinofuranoside, as previously described (Losi *et al.* 2002), to facilitate formation of a synaptic network. Cultured neurons were transfected at DIV 7 with WT α1 or T258F α1 and GFP plasmids with a calcium phosphate protocol. Recordings were performed starting from DIV 10. The perfusion solution contained the following (in mM) 119 NaCl, 2.5 KCl, 1.3 Na$_2$SO$_4$, 2.5 CaCl$_2$, 26.2 NaHCO$_3$, 1 NaH$_2$PO$_4$, 22 glucose, and was continuously gassed with 95% O$_2$–5% CO$_2$, pH 7.35, osmolarity 290–298 mOsm.

To assess modulation of synaptic efficacy in polysynaptic signalling pathways, we used experimental approach tested on cell cultures previously (Bi & Poo, 1999). Briefly, evoked excitatory postsynaptic currents (eEPSCs) were recorded from the neuron in a network of 20–30 cells (cut from surrounding cell culture with a blunt electrode) after current injection applied to another patched neuron nearby. For the sake of clarity, we isolated segments of neuronal networks containing only one GFP-fluorescent cell, which was recorded when transfection with the human WT or T258F α1 subunit was studied, or no GFP-fluorescent cells in control. Perfusion solution in this experiment did not contain neural receptor antagonists. Each eEPSC component propagated by recorded neuron was interpreted as a signal delivered through a separate polysynaptic pathway with a specific transmission delay. To quantify the impact of GlyRs on synaptic efficacy, we measured the probability of eEPSC component occurrence (P) in control and after a series of paired stimuli. To allow registration of both increase and decrease of P, at the beginning of the experiment, stimulation was adjusted to generate P in an interval $25\% < P < 75\%$. If under control conditions the eEPSC component had P outside of this interval, the component was not used in further statistical calculations. Analysis

of current transients activated by $+5$ mV voltage steps in voltage-clamp mode gave 2.93 ± 0.11 pS as a value of CGC membrane capacitance ($n = 186$), which resembles earlier observations (D'Angelo *et al.* 1995; Hevers & Lüddens, 2002).

Data analysis

Analysis of the macroscopic currents. Continuous application of GlyR ligands evoked macroscopic responses, where 'stable' response was determined as a difference between average value of baseline (2–3 s interval before ligand(s) application) and stable current generated at a 5–10 s interval after stabilization of recording current after ligand(s) application.

Analysis of concentration–response relationships. Concentration–response curve fitting for changes of response amplitude (A_{GlyR}) was performed with a Hill equation

$$A_{GlyR} = \frac{C^{n_H}}{EC_{50} + C^{n_H}}$$

for agonists, and

$$A_{GlyR} = 1 - \frac{C^{n_H}}{EC_{50} + C^{n_H}}$$

for strychnine, where C is a ligand concentration, EC_{50} is the concentration which causes half-maximum effect and n_H is Hill's coefficient.

Analysis of phasic responses. Decay profiles of phasic responses were fitted with an exponential function

$$\Delta I = -a e^{\frac{-t}{\tau}}$$

where ΔI is a difference between current recorded at baseline and at time t, e is Euler's constant, a is a fitting constant and τ is the decay time constant.

Analysis of the single-channel recordings. Application of GlyR agonists at outside-out patches evoked single-channel openings to several conductance levels. Therefore, to calculate and visualize average GlyR conductance characteristics, we constructed all-points histograms and fitted them with a multi-Gaussian function:

$$F = \frac{p_1 e^{-\frac{(n-m_1)^2}{2\sigma_1^2}}}{\sigma_1 \sqrt{2\pi}} + \frac{p_2 e^{-\frac{(n-m_2)^2}{2\sigma_2^2}}}{\sigma_2 \sqrt{2\pi}} + \cdots + \frac{p_k e^{-\frac{(n-m_k)^2}{2\sigma_k^2}}}{\sigma_k \sqrt{2\pi}},$$

where k is a number of peaks at a histogram, m_1, m_2 … m_k are the mode values of Gaussians, σ_1, σ_2 … σ_k are the standard deviations of corresponding modes, n is the value of electrical current, p_1, p_2 … p_k are the fitting constants and e is Euler's constant. The general algorithm of multi-Gaussian histogram construction, fitting and interpretation was adapted from the work of Bennett & Kearns (2000) and Traynelis & Jaramillo (1998).

To quantify input of each conductance level into overall charge transfer, we first obtained a value of the overall charge transfer as a sum of dot values (ΣI_o) in recorded traces for which the true inequality is $I_o \le I_{m1} + 2I_{\sigma1}$, where I_o is a (negative) current recorded when GlyR is in an open state, I_{m1} is a (negative) current which corresponds to the smallest conductance peak of the multi-Gaussian fitting function, and $I_{\sigma1}$ is a (positive) current value which corresponds to the value of the standard deviation of the smallest conductance peak. Next, we obtained charge transfer for each conductance level as a sum of dot values (ΣI_c) in recording trace for which the true inequality is $I_c + 2I_{\sigma c} \ge I_c \ge I_c - 2I_{\sigma c}$, where I_c is the current which corresponds to the Gaussian peak at a certain conductance level, and $I_{\sigma c}$ is the current value which corresponds to the value of the standard deviation of this Gaussian peak. Part of each conductance level in an overall charge transfer was then calculated as $\Sigma I_c / \Sigma I_o \times 100\%$. Single channel openings to certain conductance were selected automatically by the threshold-detection algorithm of Clampfit software with a minimum event time length of 0.2 ms.

For the semi-quantitative assessment of amount of GlyR agonists released from cerebellar tissue in response to high-frequency stimulation in a sniffer patch experiment, we used an open time fraction of single-channel patch recording. This was calculated as a ratio t_o/t_c, where t_o is the full time of a given recording when GlyR(s) in a patch were in the open state and t_c is the time when GlyR(s) were in closed state.

Analysis of tonic currents. For analysis of tonic whole-cell currents, mean values of holding current were averaged at 30 s intervals. The shift of the tonic current was calculated as the difference between the holding current values (ΔI_{hold}) measured at stable baseline intervals before and after the application of 1 μM strychnine.

CGP-55845, S-MCPG, strychnine, MDL-72222, picrotoxin, tetrodotoxin, bicuculline and pentylenetetrazole were purchased from Tocris Bioscience (Abingdon, UK). APV, NBQX and QX-314 were purchased from Alomone Labs (Jerusalem, Israel). Cell culture media, trypsin, bovine calf serum and antibiotics were purchased from Thermo Fisher Scientific (Waltham, MA, USA). All other chemicals were purchased from Sigma-Aldrich (Gillingham, Dorset, UK). The WTα1 GlyR plasmid and GFP plasmid were kindly donated by Prof. Peter Schofield from the Garvan Institute, Sydney; the T258Fα1 plasmid was kindly donated by Prof. Joseph Lynch from the University of Queensland, Brisbane. The α2 and β GlyR plasmids were purchased from OriGene (Rockville, MD, USA).

Table 1. Pharmacology of GlyRs of different subunit composition expressed in HEK-293 cells

GlyR subunit composition	Glycine			β-Alanine			Strychnine *vs.* glycine*			Strychnine *vs.* β-alanine*		
	EC_{50} (μM)	n_H	n	EC_{50} (μM)	n_H	n	IC_{50} (nM)	n_H	n	IC_{50} (nM)	n_H	n
WTα1	32.3 $\pm$ 2.1 (26.1 $\pm$ 17.3)	2.6 $\pm$ 0.3	6	267 $\pm$ 43.8 (318 $\pm$ 141)	2.3 $\pm$ 0.2	6	8.7 $\pm$ 1.8 (13.2 $\pm$ 6.4)	1.9 $\pm$ 0.6	6	7.6 $\pm$ 1.3 (9.6 $\pm$ 1.8)	2.2 $\pm$ 0.2	5
T258Fα1	6.8 $\pm$ 1.1 (11.3 $\pm$ 6.2)	1.7 $\pm$ 0.2	6	70 $\pm$ 13.2 (92.3 $\pm$ 48.6)	1.8 $\pm$ 0.3	6	52.6 $\pm$ 8.7 (39.5 $\pm$ 19.8)	2.3 $\pm$ 0.5	6	34.1 $\pm$ 7.4 (22.5 $\pm$ 11.7)	2.4 $\pm$ 0.5	6
WTα1β	18.8 $\pm$ 2.9 (13.8 $\pm$ 8.7)	2.2 $\pm$ 0.2	7	142 $\pm$ 14.1 (206 $\pm$ 117)	2.2 $\pm$ 0.4	5	10.3 $\pm$ 2.1 (24.1 $\pm$ 16.7)	2.1 $\pm$ 0.7	6	7.4 $\pm$ 1.6 (8.3 $\pm$ 4.3)	2.0 $\pm$ 0.4	6
T258Fα1β	8.1 $\pm$ 0.9 (14.1 $\pm$ 7.6)	1.5 $\pm$ 0.1	6	77 $\pm$ 12.8 (104 $\pm$ 56.4)	1.9 $\pm$ 0.3	7	59.8 $\pm$ 8.6 (88.3 $\pm$ 36.2)	2.6 $\pm$ 0.7	5	42.6 $\pm$ 8.9 (31.4 $\pm$ 11.9)	2.1 $\pm$ 0.3	5

Data are means $\pm$ SEM for whole-cell recordings. Values calculated for equilibrated current; EC_{50} and IC_{50} values obtained for peak current are given in parentheses. *Agonist concentration equals EC_{50} obtained when pure agonist (glycine or β-alanine) was tested at GlyRs of corresponding subunit composition.

All data are shown as the mean $\pm$ SEM. Two-way and one-way analysis of variance (ANOVA) with a Tukey *post hoc* test, and Student's paired and unpaired *t* test were used for statistical calculations as indicated. Non-linear fitting and related statistical calculations were performed with the Mathematica 11 software package (Wolfram, Champaign, IL, USA).

Results

Effect of T258F mutation and GlyR subunit composition on affinity to ligands

Initially, dose–response dependencies for GlyR ligands with T258F and WT GlyRs were tested, with EC_{50} (or IC_{50} for strychnine *vs.* agonist) and Hill coefficient (n_H) as quantitative readouts (refer to Tables 1 and 2 for numerical values).

Increasing concentrations of Gly and Ala were first applied to HEK-293 cells expressing homomeric (α1) and heteromeric (α1β) GlyRs, and two-way ANOVA with a Tukey *post hoc* test was used for the data analysis. When we measured the effect on peak current, obtained values had high variability and thus were hardly interpretable (Table 1). The possible explanation for this phenomenon is an initial turbulence in applied solution that activates neighbouring cells, which then transfer an electrical signal to the recorded cell. This transfer is enabled by gap junctions (which connect >90% of abutting HEK cells) and tunnelling nanotubes (which connect ~50% of distant HEK cells) (Wang *et al.* 2010). Additionally, in some recordings, maximum current amplitude was observed for stabilized (equilibrated) effect (these recordings were not used in statistical calculations). Hence, for the whole-cell recordings we took measurements at a time interval where the effect was already equilibrated (Fig. 1A–D). Here and in further experiments we used for purposes of ANOVA

an agonist (Gly or Ala) as the independent factor 1 and a GlyR subunit composition as the independent factor 2.

We found that EC_{50} for Ala was significantly higher than for Gly, but no significant difference between agonists was observed for generated n_H. GlyR subunit composition also exerted a significant impact on EC_{50} values: presence of β subunit or T258F α1 subunit lowered an agonist's EC_{50}; however, only presence of T258F α1 subunit, but not β subunit, made a significant impact on n_H (see Table 1 and Fig. 1A, B, I and J). Two-way ANOVA on values of EC_{50}: factor 1: $F_{1,41} = 16.31$, $P = 2 \times 10^{-4}$; factor 2: $F_{3,41} = 10.37$, $P = 3.3 \times 10^{-5}$, Tukey test: $P > 0.05$ for T258Fα1 *vs.* T258Fα1β; for factor 1 $\times$ factor 2: $F_{3,41} = 3.18$, $P = 0.034$. Two-way ANOVA on values of n_H: factor 1: $F_{1,41} = 2.78$, $P = 0.103$; factor 2: $F_{3,41} = 6.12$, $P = 0.0015$, Tukey test: $P > 0.05$ for WTα1 *vs.* WTα1β and for T258Fα1 *vs.* T258Fα1β; factor 1 $\times$ factor 2: $F_{3,41} = 2.42$, $P = 0.08$.

Next, we studied the strychnine (Str) effects on WT and T258F GlyRs against the previously found EC_{50} of agonists. Here the presence of the T258Fα1 subunit significantly increased the IC_{50} values of Str, whereas the presence of the β subunit did not make a significant impact; no significant difference between Gly and Ala in terms of counteracting Str effect was found. Neither subunit composition nor type of agonist induced a significant bias of n_H (Table 1 and Fig. 1C, D, K and L). Two-way ANOVA on IC_{50} data: factor 1, $F_{1,37} = 2.56$, $P = 0.118$; factor 2, $F_{3,37} = 7.92$, $P = 3.3 \times 10^{-4}$, Tukey test: $P > 0.05$ for WTα1 *vs.* WTα1β and for T258Fα1 *vs.* T258Fα1β; factor 1 $\times$ factor 2: $F_{3,37} = 2.09$, $P = 0.118$. Two-way ANOVA on n_H values: $P > 0.1$ for both factors.

Whole-cell recordings from HEK cells confirmed the pharmacological profile of GlyRs expressed from our plasmids. As the next step, we set out to test whether pharmacological properties of expressed GlyRs are similar in different cultured cell types (HEK and CGC) and in CGCs of living tissue. Our working hypothesis was

Table 2. Pharmacology of GlyRs of different subunit composition expressed in HEK-293 cells and in CGCs

GlyR subunit composition, cell type	Glycine			Strychnine *vs.* glycine*		
	EC_{50} (μM)	n_H	n	IC_{50} (nM)	n_H	n
WTα1β, HEK	20.3 $\pm$ 1.8	1.9 $\pm$ 0.1	5	8.4 $\pm$ 1.8	2.0 $\pm$ 0.4	5
T258Fα1β, HEK	7.9 $\pm$ 1.2	1.4 $\pm$ 0.2	5	49.6 $\pm$ 7.6	2.8 $\pm$ 0.5	5
WTα1, CGC	21.2 $\pm$ 1.9	2.1 $\pm$ 0.2	5	7.8 $\pm$ 2.2	1.9 $\pm$ 0.3	5
T258Fα1, CGC	8.5 $\pm$ 0.6	1.7 $\pm$ 0.3	6	52.6 $\pm$ 4.3	2.2 $\pm$ 0.2	5
Living tissue, CGC	24.5 $\pm$ 3.2	2.3 $\pm$ 0.4	5	9.3 $\pm$ 2.9	2.2 $\pm$ 0.4	5

Data are means $\pm$ SEM for recordings from nucleated patches. Values calculated for peak current. *Glycine concentration equals EC_{50} obtained when pure glycine was tested at GlyRs of corresponding subunit composition.

as follows: α1 subunits expressed in CGCs mainly generate heteromeric GlyRs with β subunits naturally expressed in this cell type. Therefore, the pharmacological profile of GlyRs in CGCs transfected with WTα1 and T258Fα1 plasmids should be similar to that of WTα1β- and T258Fα1β-transfected HEK cells, respectively. As a consequence, the pharmacological profile of CGCs in living tissue should be similar to WTα1β-transfected HEK cells.

To obtain a more controlled experimental environment, we first tried to apply Gly and Gly+Str at outside-out membrane patches instead of whole cells. The vast majority of outside-out patches excised from both cultured CGCs and CGCs of cerebellar brain slices (8 out of 11 tried) after application of Gly displayed single-channel openings rather than a poly-receptor response of the kind that was observed in the whole-cell mode. However, when we repeated the experiment with nucleated patches, the poly-receptor response was generated in all trials (see example traces in Fig. 1*E*–*H*). Values of Gly EC_{50}, Str IC_{50} and n_H obtained for peak current in nucleated patches were similar to those of HEK cells transfected with WTα1β, cultured CGCs transfected with WTα1, CGCs from living tissue, and WTα1β-transfected HEK cells recorded in whole-cell mode: $P > 0.3$ for all comparisons, $n = 10$–13, Student's *t* test. Another set of similar readouts was obtained for nucleated patches from T258Fα1β-transfected HEK cells, T258Fα1-transfected CGCs and T258Fα1β-transfected HEK cells in whole-cell mode: $P > 0.2$ for all comparisons, $n = 10$–12, Student's *t* test; see Tables 1 and 2 for numerical data. These results support our working hypothesis and thus confirmed similar pharmacological profiles of GlyRs expressed in cell cultures and in living tissue.

Effect of T258F mutation and GlyR subunit composition on receptor conductance

As the next step, we tested the mutation effect on GlyR single-channel electrical conductance in outside-out patches excised from HEK cells (Fig. 2; see Table 3 for

numerical data). Here we applied the lowest agonist concentration which exerted a significant effect in a whole-cell experiment on the corresponding type of GlyR (Fig. 1). We found that all-point histograms for homomeric receptors are best-fitted with three Gaussians, indicating three main conductance states, whereas the presence of a β subunit reduced the number of conductance states to two (Fig. 2*C* and *D*). For all GlyR subunit compositions, the highest conductance state delivered >85% of the overall charge transfer (Table 3). Therefore, to assess the influence of agonists and GlyR subunit composition on GlyR conductance, we analysed data on the openings to highest conductance. We found that the presence of both T258F α1 subunit and β subunit lowers the highest conductance level, whereas no significant difference in this GlyR characteristic was observed when Ala or Gly was applied. Two-way ANOVA output: factor 1, $F_{1,44} = 1.37$, $P = 0.25$; factor 2, $F_{3,44} = 5.12$, $P = 0.004$, Tukey test: $P > 0.05$ for WTα1β *vs.* T258Fα1β; factor 1 $\times$ factor 2: $F_{3,44} = 2.61$, $P = 0.063$.

To compare single-channel characteristics of GlyRs expressed in HEK cells to those expressed in CGCs, we repeated the experiment on outside-out patches excised from cultured CGCs transfected with WTα1 and T258Fα1 plasmids, and from CGCs of living tissue (Table 4). In all three experiments on CGCs, single-channel GlyR conductance had no significant difference from values obtained when WTα1β and T258Fα1β receptors were expressed in HEK cells: $P > 0.2$ for all comparisons, $n = 12$, Student's *t* test (see Tables 3 and 4).

GlyR subunit composition shapes response kinetics

For deeper analysis of GlyR functional properties, we next studied the decay kinetics of response evoked by brief ($\sim$200 μs) applications of 50 μM Gly and 500 μM Ala in membrane patches carrying GlyRs of different types. This experiment again demonstrated the significant impact of both agonist species and GlyR subunit composition on the response kinetics (Fig. 3). To quantify this impact, we used values of decay time constant (τ) obtained with a

non-linear fitting of response decay profiles. Responses generated by Gly displayed significantly slower decay (higher decay τ) than responses generated by Ala; the presence of the β subunit, but not the T258Fα1 subunit made decay faster, i.e. lowered τ values. Two-way ANOVA results for τ values: for factor 1: $F_{1,40} = 205$, $P = 2.5 \times 10^{-17}$; for factor 2: $F_{3,40} = 24.6$, $P = 3.5 \times 10^{-9}$, Tukey test: $P > 0.05$ for WTα1 *vs.* T258Fα1; for factor 1 $\times$ factor 2: $F_{3,40} = 9.6$, $P = 6.6 \times 10^{-5}$.

To test whether results obtained for GlyRs expressed in HEK cells are applicable to CGCs, we repeated this experimental protocol at nucleated patches excised from cultured CGCs in control (no additional transfection), CGCs transfected with WTα1 plasmid, and CGCs transfected with T258F plasmid, applying 50 μM Gly (Fig. 3E and F). We found that transfection with T258Fα1, but not with WTα1, slows significantly the response decay kinetics when compared to control. For T258Fα1 *vs.* control: $P = 0.004$, $n = 12$; for WTα1 *vs.* control: $P = 0.39$, $n = 12$, Student's *t* test. This result reproduces an observation for HEK cells transfected with T258Fα1$+\beta$ and WTα1$+\beta$ (Fig. 3A and B). Hence it is in line with the presumption
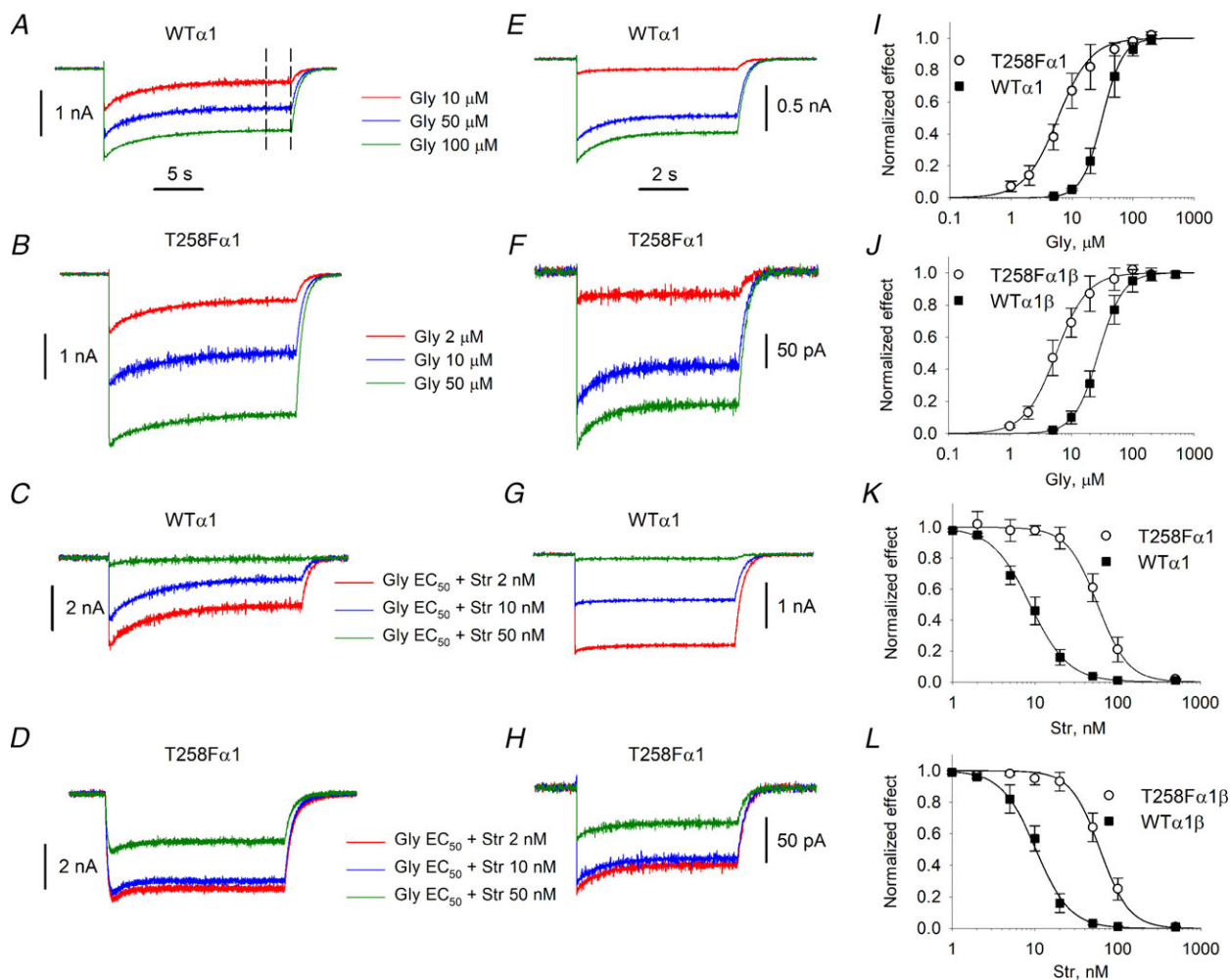

Figure 1. Affinity of GlyRs of different subunit composition to GlyR ligands
A–D, example whole-cell responses recorded from HEK-293 cells. Dashed lines in *A* denote the interval where response amplitude was measured. *A*, transfection with WTα1 GlyR, effect of increasing concentrations of glycine. *B*, transfection with T258Fα1 GlyR, effect of increasing concentrations of glycine. *C*, transfection with WTα1 GlyR, effect of increasing concentrations of strychnine applied together with stable concentration of glycine. *D*, transfection with T258Fα1 GlyR, effect of increasing concentrations of strychnine applied together with stable concentration of glycine. *E–H*, example traces recorded from nucleated patches of cultured cells. *E*, same as *A*, nucleated patch from HEK cell. *F*, same as *B*, nucleated patch from CGC. *G*, same as *C*, nucleated patch from HEK cell. *H*, same as *D*, nucleated patch from CGC. Colour codes in *A–H* apply to sets of traces where similar solutions were used (traces to left and to right of corresponding legend). *I–L*, example concentration–response plots for GlyR ligands with Hill's equation fitting curves; response amplitudes are normalized to maximum response. Strychnine effect was studied against EC$_{50}$ of glycine obtained in experiments on GlyR of similar subunit composition. Refer to Tables 1 and 2 for numerical data on effects of all tested ligands at all GlyR types. [Colour figure can be viewed at wileyonlinelibrary.com]
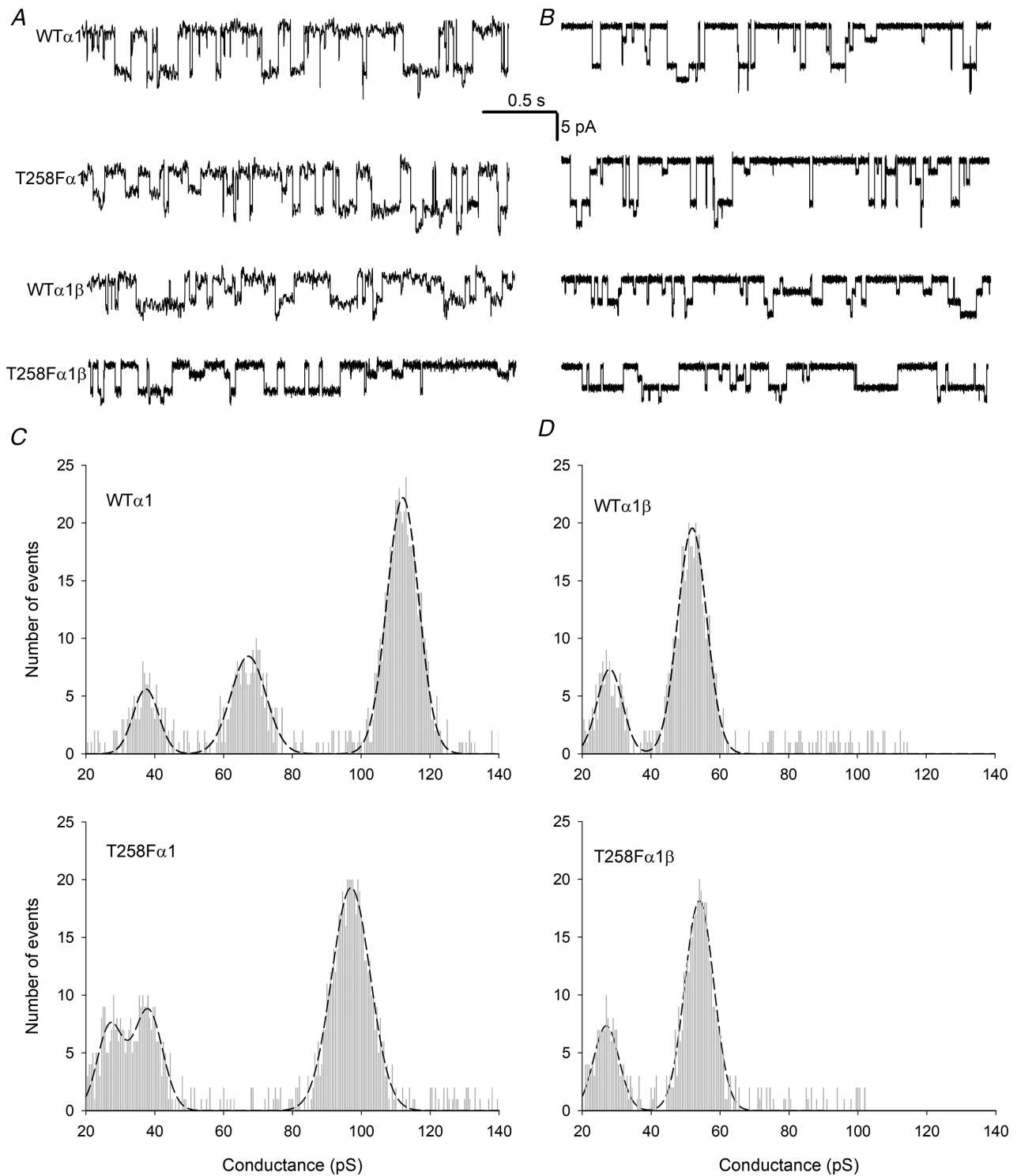
Figure 2. Single-channel currents generated by GlyRs of different subunit composition
A, single-channel responses triggered by glycine application. *B*, single-channel responses triggered by β-alanine application. From top to bottom: homomeric WTα1 GlyR, homomeric T258Fα1 GlyR, heteromeric WTα1β GlyR, heteromeric T258Fα1β GlyR. Each receptor subtype activated by EC_{50} of corresponding ligand obtained in experiment on whole cell currents. Scale bars and trace labels apply to *A* and *B*. *C*, example all-point histograms of single-channel conductances obtained for homomeric GlyRs. Top, WTα1 GlyR. Bottom, T258Fα1 GlyR. *D*, example all-point histograms of single-channel conductances obtained for heteromeric GlyRs. Top, WTα1β GlyR. Bottom, T258Fα1β GlyR. Refer to Table 3 for numerical data on subconductance levels revealed by Gly and Ala for different subunit compositions.

Table 3. Conductance states and their input into overall charge transfer for GlyRs expressed in HEK-293 cells and recorded from outside-out patches

	Agonist			
	Glycine		β-Alanine	
GlyR subunit composition	Conductance states (pS)	Charge transfer (%)*	Conductance states (pS)	Charge transfer (%)*
WTα1	112 ± 3.6, 67 ± 1.8, 37 ± 2.4	86.2, 9.7, 3.3	108 ± 2.2, 71 ± 2.3, 32 ± 2.7	87.3, 8.4, 2.2
T258Fα1	97 ± 2.9, 38 ± 4.1, 27 ± 3.3	92.1, 2.8, 4.8	95 ± 1.4, 46 ± 2.8, 19 ± 2.7	91.3, 2.5, 5.1
WTα1β	52 ± 1.9, 28 ± 2.6	88.6, 8.8	56 ± 2.8, 25 ± 2.7	92.7, 5.4
T258Fα1β	54 ± 2.5, 27 ± 1.7	90.3, 7.9	51 ± 3.1, 29 ± 2.3	89.6, 8.2

Data are means ± SEM. Agonists concentration equals EC_{50} obtained in whole cell for corresponding subunit composition; $n = 6$ for glycine, $n = 7$ for β-alanine. *Sum of values may be <100% due to high-amplitude noise events.

Table 4. Conductance states and their input into overall charge transfer for GlyRs expressed in CGCs and activated by glycine in outside-out patches

GlyR subunit composition	Conductance states (pS)	Charge transfer (%)*
Transfected with WTα1	56 ± 2.6, 30 ± 2.2	94.8, 4.6
Transfected with T258Fα1	51 ± 3.1, 28 ± 2.3	87.2, 9.1
Living tissue	57 ± 1.8, 29 ± 3.1	90.1, 8.8

Data are means ± SEM. For WTα1 and T258Fα1 overexpressed in cultured CGCs, glycine concentration equals EC_{50} obtained in HEK-293 cells for corresponding subunit composition. Data for living tissue were obtained in a sniffer patch experiment, $n = 6$ for all experiments. *Sum of values may be < 100% due to high-amplitude noise events.

that, being transfected with WTα1, the CGCs generate heteromeric WTα1β GlyRs, similar to native GlyRs of CGCs and to those generated in HEK cells transfected with WTα1+β plasmids. In turn, transfection of CGCs with T258Fα1 results in a mixture of heteromeric T258Fα1β and WTα1β GlyRs.
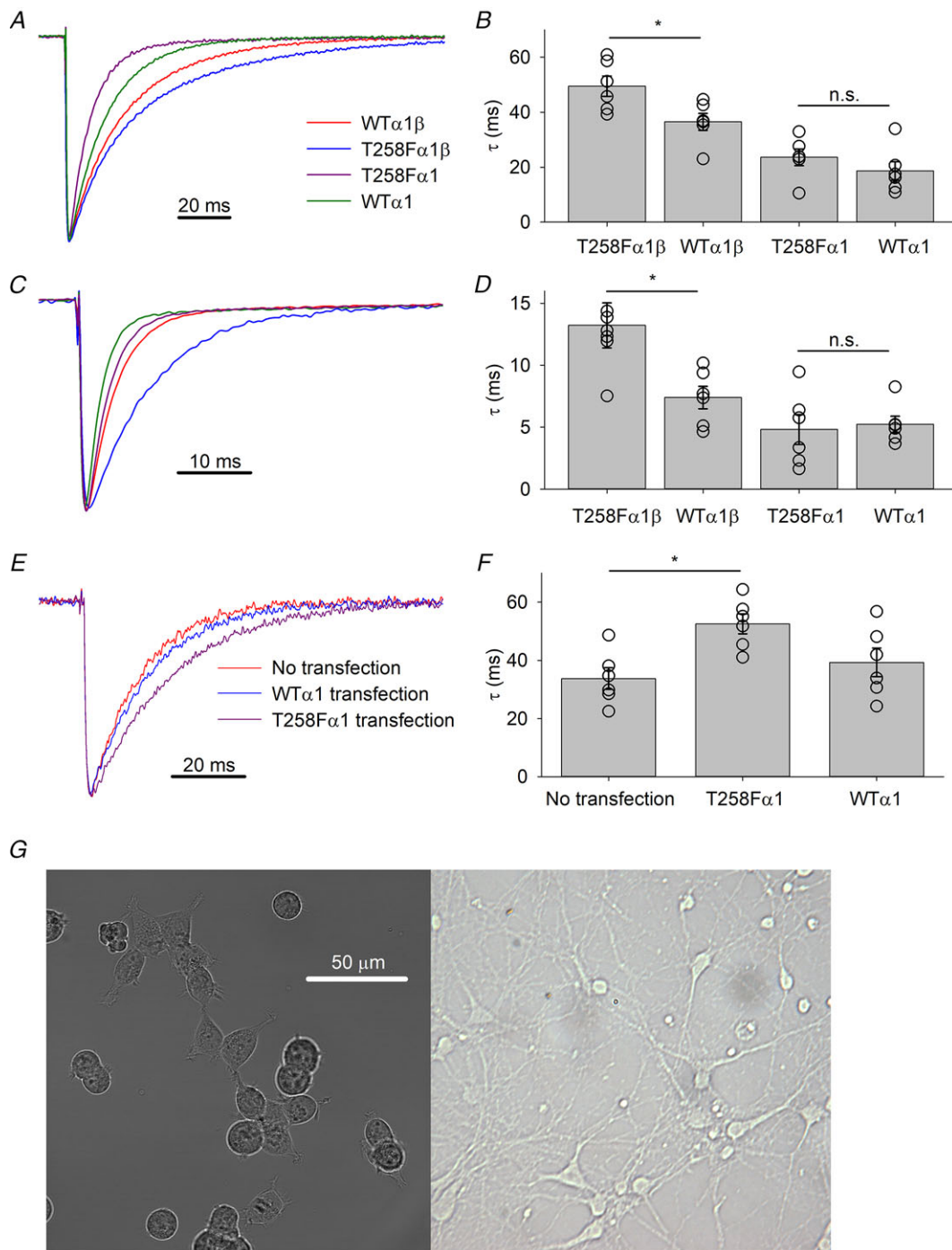
GlyR sensitivity to GABA$_A$R open-channel blockers

Single-receptor recordings revealed two different modes of the main conductance state: ~100–110 pS for HEK cells transfected with WTα1 and T258Fα1 and ~50–60 pS for WTα1β- and T258Fα1β-transfected HEK cells, WTα1- and T258Fα1-transfected CGCs, and CGCs of living tissue (Tables 3 and 4). This pattern suggests that (i) α1 subunits expressed from transfected DNA form heteromeric GlyRs with wild-type β subunits when they are present in a given cell, and (ii) properties of these receptors are similar to those in CGCs of acute tissue.

To further confirm this finding and to test whether GABA$_A$R open-channel blockers such as picrotoxin (PTX) and pentylenetetrazole (PTZ) do not affect heteromeric GlyR functioning in our preparation, we performed an additional solution exchange experiment on nucleated patches. In this experiment each patch underwent application of 10 μM Gly and then 10 μM Gly+10 μM PTX, or 10 μM Gly+1 mM PTZ (Fig. 4). PTX, being applied at patches from WTα1-transfected HEK cells, lowered the response amplitude to 0.42 ± 0.16 of control: $P = 0.022$, $n = 6$, Student's paired t test. For all other sets of plasmids expressed in both HEK cells and CGCs, and for nucleated patches from CGCs of living tissue, PTX and PTZ did not display a significant effect: $P > 0.3$, $n = 6$ for all cases, Student's paired t test (Fig. 4D). PTX, displaying a significant effect exclusively at homomeric WTα1 receptors, confirmed earlier observations (Pribilla *et al.* 1992; Shan *et al.* 2001). Hence, we obtained an additional confirmation of heteromeric composition of GlyRs in all cell types where the β GlyR subunit is expressed. In turn, 1 mM PTZ did not exert a significant effect on any GlyR type (in accord with earlier studies; see Corda *et al.* 1991), thus enabling us to use it for silencing of GABA$_A$Rs in further experiments on living tissue with presumed GABA spillover.

As an additional control on subunit composition of GlyRs in CGCs, we tested the antagonist effect of bicuculline (BIC) on α1β and α2β GlyRs expressed in HEK cells and on GlyRs from CGCs of acute tissue. BIC at 1 mM, when applied against 60 μM of Gly, was shown to block in full the conductance generated by α2β GlyRs, but not by α1β GlyRs (Li & Slaughter, 2007). We repeated this experimental protocol to find that 1 mM BIC indeed fully suppressed the effect of α2β GlyRs in HEK cells (response amplitude 0.045 ± 0.007 of control), but not α1β GlyRs in HEK cells and GlyRs from CGCs of acute tissue: 0.392 ± 0.096 and 0.43 ± 0.089 for HEK cells and CGCs, respectively (Fig. 4C and E). This result confirmed that α1-containing GlyRs generate at least a significant part of the GlyR effect in CGCs of 25- to 30-day-old C57Bl-6J mice and provided the rationale for the α1 overexpression experiments.

Figure 3. T258F mutation slows kinetics of GlyR response triggered by brief application of agonists
A, GlyR responses evoked in HEK cell outside-out membrane patches by ~200 μs application of 1 mM glycine. Trace colour codes apply to *A* and *C*. *B*, statistical summary of *A*, decay time constant (τ) values of response generated by GlyRs of different subunit composition after glycine application. In *B* and *D* response amplitudes were normalized to those of WTα1 receptor. *C*, GlyR responses evoked in HEK cell outside-out membrane patches by ~200 μs application of 5 mM β-alanine. *D*, statistical summary of *C*, τ values of responses generated by GlyRs of different subunit composition after β-alanine application. *E*, GlyR responses evoked in CGC nucleated patches by ~200 μs application of 1 mM glycine. Response traces are normalized to peak current in non-transfected cell. *F*, statistical summary of *E*, τ values of response generated by GlyRs of different subunit composition after glycine application. *G*, images of cultured HEK cells (left) and CGCs (right). Scale bar: 100 μm, applies to both images. *P < 0.05, n = 6, Student's *t* test. [Colour figure can be viewed at wileyonlinelibrary.com]

GlyR input into tonic conductance in living neural tissue

Previous experiments allowed us to assess the influence of mutant GlyR subunits on single-channel properties, and on poly-receptor response parameters in an artificial expression system (HEK cells) as well as in cultured CGCs and CGCs from acute slices. Therefore, in the next stage of the research we decided to test the GlyR impact on inter-neuronal signalling in living cerebellar tissue.

As a first step, we clarified whether GlyR conductance has a significant input into neural tonic signalling in cerebellar vermis. To achieve this, we performed a continuous whole-cell recording from CGCs in vermis slices (Fig. 5). To isolate GlyR activity we added a cocktail of ligands (including PTZ), which blocked all other receptors (see 'Cerebellar acute slices' section of Methods for more details). GlyR response-isolating ligands fully suppressed spontaneous activity in CGCs. However, subsequent applications of 1 μM strychnine did not induce

any significant effect, shifting the holding current by 1.57 ± 0.84 pA; the significance of the difference from zero was $P = 0.103$, $n = 8$, Student's t test (Fig. 5A and D). We therefore repeated the experimental protocol, adding high-frequency stimulation (HFS): eight bursts of 10 impulses at 100 Hz delivered to mossy fibres (D'Angelo *et al.* 1999) 10 min before drug application. After HFS, application of strychnine following GlyR-isolating ligands revealed the presence of GlyR-mediated tonic conductance of 5.38 ± 0.82 pA, thus proving the presence of functional tonically active GlyRs; the significance of the difference from zero was $P = 3.1 \times 10^{-4}$, $n = 8$, Student's paired t test (Fig. 5A and D).

We next asked, what is the mechanism revealing GlyR-mediated tonic conductance after HFS? The simplest explanation is that HFS upregulates the synaptic vesicular release, which results in neurotransmitter spillover and, as a consequence, results in an increase of neurotransmitters (in particular Gly) concentration in extracellular space. To test this hypothesis, we repeated the experiment without
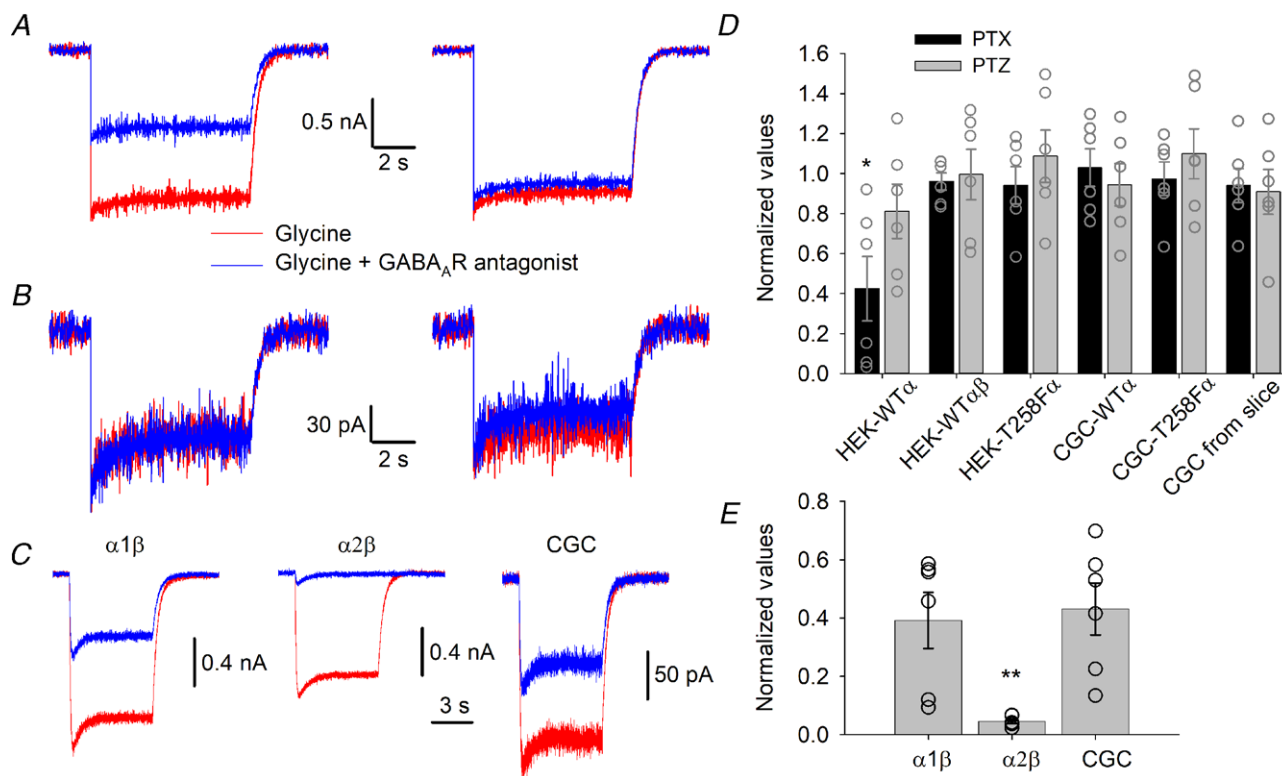

Figure 4. GlyR subunit composition determines response to GABA$_A$-receptor antagonists
A and *B*, example traces illustrating effect induced in nucleated patches by application of 10 μM glycine and glycine+GABA$_A$R antagonists. *A*, WTα1 subunit expressed in HEK cells. *B*, CGC of acute tissue. For *A* and *B*, left, effect of 10 μM picrotoxin (PTX); right, effect of 1 mM pentylenetetrazole (PTZ). Colour codes apply to all example traces. *C*, effect of 60 μM Gly+1 mM bicuculline (BIC) on heteromeric GlyRs of various subunit composition. Left, α1β GlyRs expressed in HEK cell. Middle, α2β GlyR expressed in HEK cell. Right, nucleated patch pulled from CGC of acute cerebellar tissue. *D*, statistical summary for *A* and *B*. Effect of Gly+PTX and Gly+PTZ on GlyR of different subunit composition expressed in HEK cells and in CGCs. Asterisk denotes significance of difference from unity. In *D* and *E* data normalized to amplitude generated by application of Gly only. *E*, statistical summary of *C*. Asterisks denote significance of difference from both α1β and CGC columns. *$P < 0.05$, **$P < 0.01$, $n = 6$, Student's t test. [Colour figure can be viewed at wileyonlinelibrary.com]
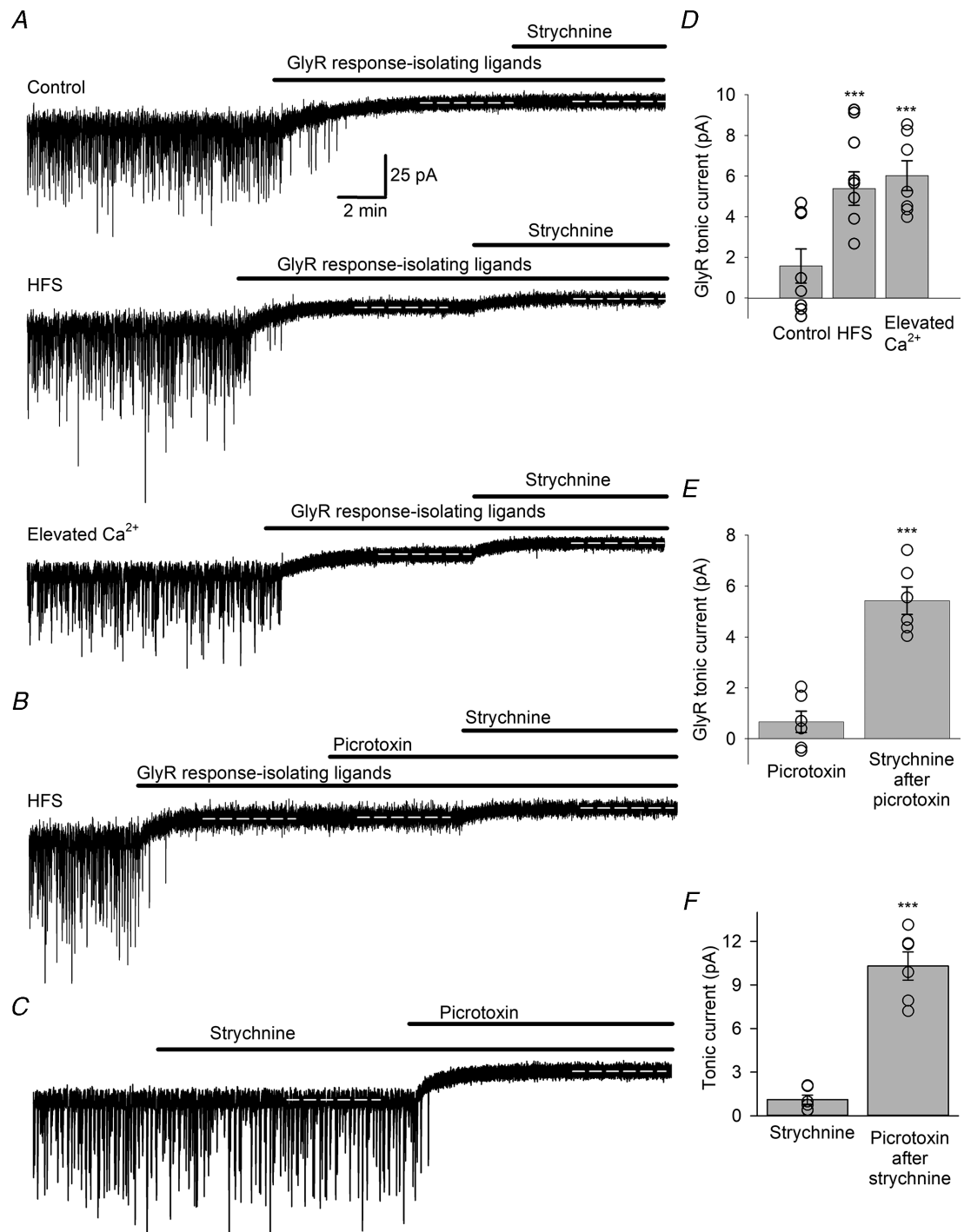
Figure 5. GlyRs generate significant tonic conductance in CGCs in response to enhanced release of neurotransmitters

A–C, example traces of whole-cell recordings from CGCs in acute tissue. Dashed lines show intervals where holding current was measured; scale bars apply to all traces. *A*, from top to bottom, under control conditions, after high-frequency stimulation (HFS, 8 bursts of 10 impulses at 100 Hz) and with elevated Ca^{2+} concentration (4 mM). *B*, GlyRs of CGC remain functional with PTX, 50 μM added to perfusion solution. *C*, strychnine does not make a significant impact on $GABA_A$Rs which are then blocked by PTX. *D*, statistical summary of *A*, changes of holding current induced by 1 μM Str. *E*, statistical summary of *B*, changes of holding current after HFS induced by 10 μM PTX and by 1 μM Str after PTX. *F*, statistical summary of *C*, changes of holding current (with no preliminary HFS) induced by Str and by PTX after Str. Asterisks denote significance of difference from zero; ***$P < 0.001$, $n = 6$–8, Student's paired *t* test.

HFS, but with Ca^{2+} concentration elevated to 4 mM, which should promote vesicle release. Indeed, under these conditions we observed a significant GlyR-mediated tonic current, similar to that after HFS: 6.02 ± 0.73 pA; the significance of the difference from zero was $P = 1.8 \times 10^{-4}$, $n = 7$, Student's paired t test (Fig. 5A, D).

Additionally, to explore whether our GlyR response-isolating cocktail fully inhibits all activity of $GABA_A$Rs, we repeated a HFS experiment, but with application of 50 μM PTX after a PTZ-containing cocktail (Fig. 5B). Under these conditions, we found no significant effect of PTX, which induced an outward shift of holding current for 0.67 ± 0.42 pA ($P = 0.53$, $n = 6$, Student's paired t test), but still a significant effect of strychnine added after PTX: 5.42 ± 0.54 pA, $P = 4.2 \times 10^{-4}$, $n = 6$, Student's paired t test (Fig. 5B, E). Next, to clarify that the impact of strychnine on holding current is not due to its side effect on $GABA_A$Rs, we performed a continuous recording experiment without HFS, when a GlyR response-isolating cocktail was not applied before strychnine, and PTX was applied after strychnine (Fig. 5C). In this experiment strychnine did not display a significant impact on holding current (difference from control 1.11 ± 0.32 pA, $P = 0.66$, $n = 6$, Student's paired t test), whereas PTX still induced a significant outward shift (difference from strychnine 10.3 ± 0.97 pA, $P = 0.0002$, $n = 6$, Student's paired t test) – see Fig. 5F.

Release of GlyR endogenous ligands in cerebellar tissue due to HFS

Next, to test directly whether cerebellar tissue releases an additional amount of GlyR agonists in a course of HFS, we combined a HFS with a sniffer patch technique (Fig. 6). To do this, we pulled an outside-out patch from a CGC, and performed a control recording of

GlyR openings at a distance of 5 μm from the slice surface. Then we repeated the recording at 300 μm above the slice. Next, we lowered the patch pipette back to 5–6 μm distance and initiated a HFS protocol; after that we again elevated the patch pipette to 300 μm distance (Fig. 6A). For quantitative assessment of the HFS effect on neurotransmitter release we calculated values of an open-time fraction which integrates single-channel open time and opening frequency (Fig. 6B). The value of the GlyR open time fraction recorded at 5 μm distance under HFS was 2.06 ± 0.26 times higher than that obtained under control conditions at the same distance ($P = 0.009$, $n = 6$, Student's paired t test). In contrast, the open time fraction was significantly lowered at a 300 μm distance when compared to that obtained at 5 μm in control: to 0.082 ± 0.031 at 300 μm under control conditions and to 0.087 ± 0.032 under HFS; $P < 0.0001$, $n = 6$ for both cases, Student's paired t test.

GlyRs of CGCs modulate action potential generation

An experiment on acute tissue has proved the presence of tonically active GlyRs in CGCs. Hence, we next asked if extrasynaptic GlyRs of CGCs modify neuronal signalling generation, and if so, how can this role be modified by the gain-of-function mutation? To clarify this, we performed experiments on cultured CGCs transfected with the T258Fα1 subunit, and WTα1 subunit as a positive control ensuring that experimental results observed in T258Fα1-expressing culture are not the side effects of the transfection procedure. The abundance of native β GlyR subunits in CGCs (brain-map.org/api/index.html) ensured the formation of heteromeric receptors in the transfected cells.

First, we studied modulatory input of tonically active GlyRs into the action potential generation. To do this, we compared the summation profile of evoked postsynaptic
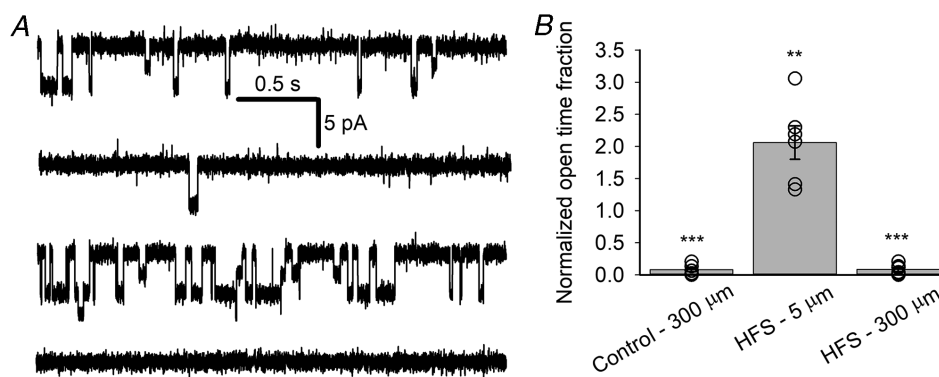

Figure 6. High-frequency stimulation induces release of GlyR ligands from acute tissue
A, example traces recorded from an outside-out sniffer patch. From top to bottom, control (no stimulation), 5 μm from slice surface; control, 300 μm from slice surface; HFS, 5 μm from slice surface; HFS, 300 μm from slice surface. B, statistical summary. Open time fraction normalized to that obtained in control at 5 μm from slice surface. Asterisks denote significance of difference from unity, **$P < 0.01$, ***$P < 0.0001$, $n = 6$, paired Student's t test.
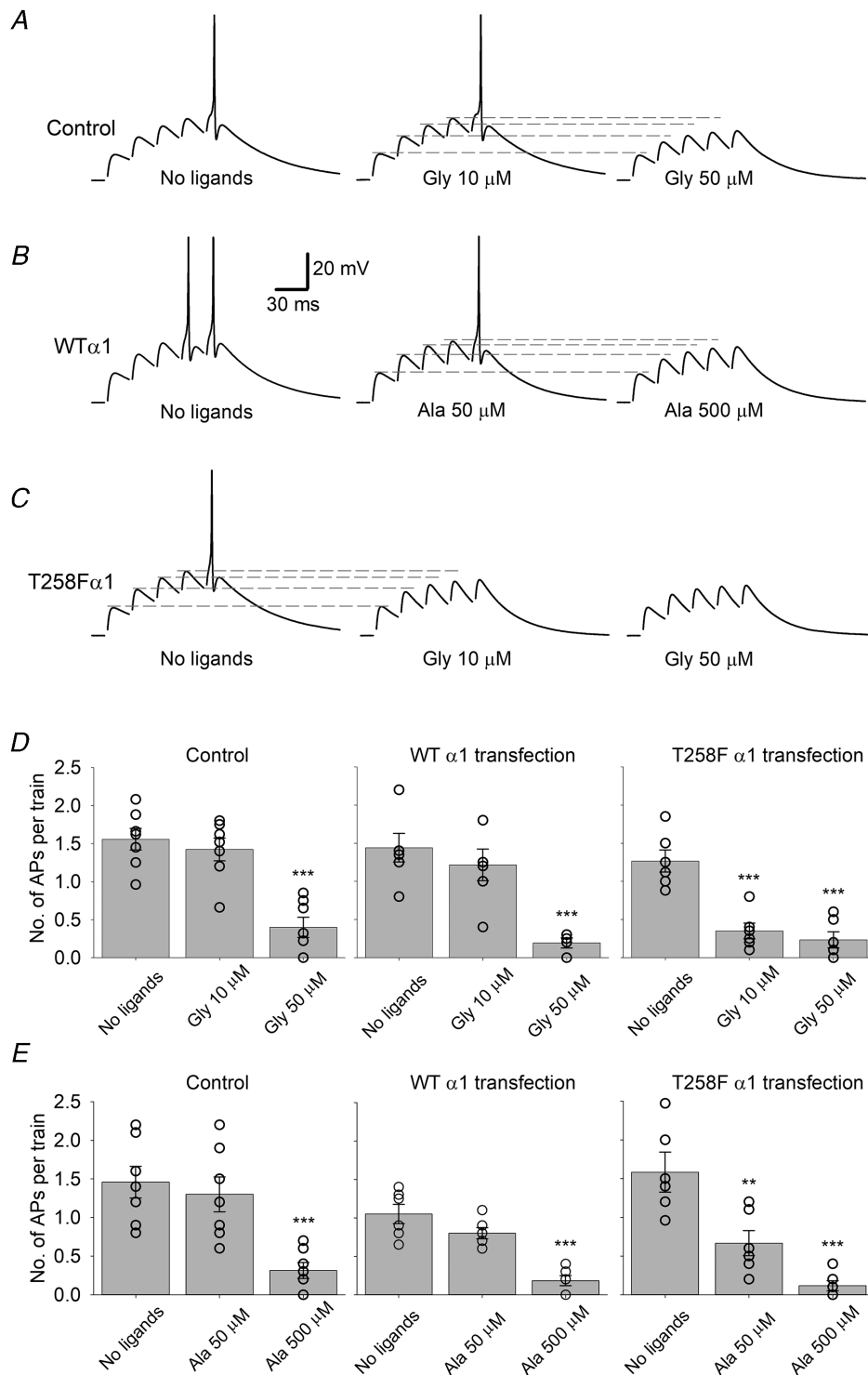
Figure 7. GlyRs modulate action potential generation in cultured CGCs
A–C, example traces illustrating EPSPs evoked in CGCs by five consecutive field stimuli in control (left) and with different concentration of GlyR agonists: low (10 μM glycine or 100 μM β-alanine, middle panel) or high (50 μM glycine or 500 μM β-alanine, right panel). Stimulation artifacts are blanked; dashed lines illustrate impact of GlyR activation on EPSP amplitude; scale bars apply to all traces in *A–C*. *A*, no transfection. *B*, WTα1 transfection. *C*, T258Fα1 transfection. *D* and *E*, statistical summary. Average number of APs generated per stimulation train in control and with different concentrations of glycine (*D*) and β-alanine (*E*). Vertical axis labels and titles on the left apply to all bar charts. Asterisks denote significance of difference from 'no ligands' value. **$P < 0.01$, ***$P < 0.001$, $n = 5$–7, Student's *t* test.

potentials (eEPSPs) during trains of five stimuli evoked by the field 50 Hz stimulation. The stimuli strength was adjusted so that, under control conditions where no GlyR ligands were added, the stimulation train induced one to three APs (Fig. 7A–C). After the control recording series (10 traces), the stimulation protocol was repeated on the same cell with low concentrations of GlyR agonist (10 μM Gly or 50 μM Ala) and then with high concentrations of agonist (50 μM Gly or 500 μM Ala), a total of 10 individual traces for each mode. The average number of APs per trace was then used for quantification of the agonist effect. The experiment was repeated for untransfected cells and cells transfected with WTα1 and with T258Fα1 cDNA. Both agonists displayed a similar response profile in untransfected CGCs and CGCs transfected with WTα1: only a high ligand concentrations exerted a significant downregulatory impact on AP numbers; on the contrary, in the case of CGCs transfected with T258Fα1, a significant decrease of AP number was generated after application of agonists in both concentrations (Fig. 7D and E).

Tonically active GlyRs modulate synaptic plasticity

An experiment on EPSP summation confirmed the significant input of GlyRs into AP generation machinery. But how could this affect the synaptic plasticity and inter-neuronal crosstalk? To address the issue, we studied networks composed of several (20–30) cultured CGCs, where two polysynaptically connected cells were patched simultaneously. Current injection into one cell generated an action potential with the subsequent poly-component eEPSC recorded from another cell. We interpreted each eEPSC component as signal transmission through separate pathways with a specific time lag. When the low-frequency stimulation (1 stimulus per 15 s) was used, the occurrence probability (P) remained stable for each eEPSC component. We thus used the eEPSC profile as a gauge allowing the quantitative measurement of synaptic efficacy (see the 'Cultured granule cells' section of Methods). To examine the synaptic plasticity in the recorded network, we applied a train of 50 paired-pulse stimuli with 50 ms inter-pulse interval at 1 Hz. After that, we monitored changes in the P (decrease or increase, i.e. ΔP) of the pre-existing eEPSC components. These changes were interpreted as an indicator of the remodelling of signalling pathways (Fig. 8A). At each recorded CGC, the experimental protocol was then repeated with low and high concentrations of agonists (similar to those used in the experiment on AP generation).

Unexpectedly, we found that 10 μM Gly increased significantly ΔP in untransfected cells and in cells transfected with WTα1, whereas a 50 μM concentration of Gly had a significant downregulatory effect. On the contrary, in the cells transfected with T258Fα1, both Gly concentrations displayed a downregulatory action

(Fig. 8D). The experiment with Ala did not display opposite effects for different concentrations: ΔP was decreased in all cases (Fig. 8C). To explain such a difference between the GlyR agonists, we hypothesized that the Gly-generated effects in this experiment were partially delivered through NMDA receptors (NMDARs) in parallel with GlyRs. To test this hypothesis, we repeated the experimental protocol with 2 nM of L-689,560, which is a high-affinity competitor for the Gly binding site of NMDAR (Grimwood *et al.* 1992), in perfusate. Indeed, under these conditions, Gly displayed an effect profile similar to that of Ala: decreased ΔP under all tested concentrations (Fig. 8E). Next, we repeated this experiment without L-689,560, but with 1 μM Str in perfusion solution (Fig. 8F). Here we found that increasing Gly concentrations elevate ΔP rather than generate a biphasic effect as at Fig. 8D. We thus concluded that Gly increases ΔP acting at NMDARs, and decreases ΔP acting at GlyRs.

Gly spillover modulates AP generation in CGCs of acute tissue

In the previous experiment we found that extrasynaptic GlyRs shape neural network functioning and can reverse the effect of glutamatergic excitatory input. However, it is unknown whether extrasynaptic GlyRs modulate CGC excitation in living tissue. To clarify this, we tested GlyRs input into the excitation machinery in cerebellar brain slices. Initially, we tried to reproduce a sensory excitatory input into a given CGC, which was shown *in vivo* to be delivered via a single mossy fibre (Chadderton *et al.* 2004). To achieve this, we used a θ-glass stimulation micro-electrode of ~5 μM diameter. With this electrode we searched for a position in the cerebellar white matter where the stimulation pulse generated eEPSC(s) in the patched CGC. Once the position was found, we delivered several groups of stimuli (5 stimuli at 25 Hz, 30 s intervals between groups); each group evoked two to five glutamatergic eEPSCs in the recorded cell, reproducing the result of *in vivo* sensory input (Chadderton *et al.* 2004). Then we compared average response amplitudes and cumulative response amplitude histograms for evoked glutamatergic eEPSCs, spontaneous eEPSCs, and mini-eEPSCs (after application of 1 μM tetrodotoxin, TTX): Fig. 9A, C and D. We found no significant difference in average response amplitude for these three eEPSC types (one-way ANOVA: $F_{2,15} = 0.47$, $P = 0.63$) and high similarity of the cumulative response amplitude histograms (Fig. 9C). The similarity of spontaneous, evoked and mini eEPSCs indicates that sensory stimulation induces bursts of responses where each is generated by a single neuro-transmitter quantum, and that our stimulation protocol resembles native sensory input delivered to an individual CGC.

Equipped with this knowledge, we then studied AP generation in response to sensory-like inputs. To do this, we used stimulation sets consisting of four groups, five stimuli at 25 Hz in each group, with 30 s inter-group intervals; after a first set, a 5 min interval was taken, and then a similar stimulation set delivered. To quantify changes in the AP-generation machinery, we used an

average number of APs generated by the five-stimuli group (Fig. 9*B*, *E* and *F*). Under control conditions, 5 min interval with no stimulation did not significantly change an average AP number: 2.93 ± 0.43 *vs.* 3.2 ± 0.28, $P = 0.48$, $n = 9$, Student's paired *t* test. To find out, whether AP generation is affected by Gly, we added 50 μM Gly after the first stimulation set. This significantly decreased a
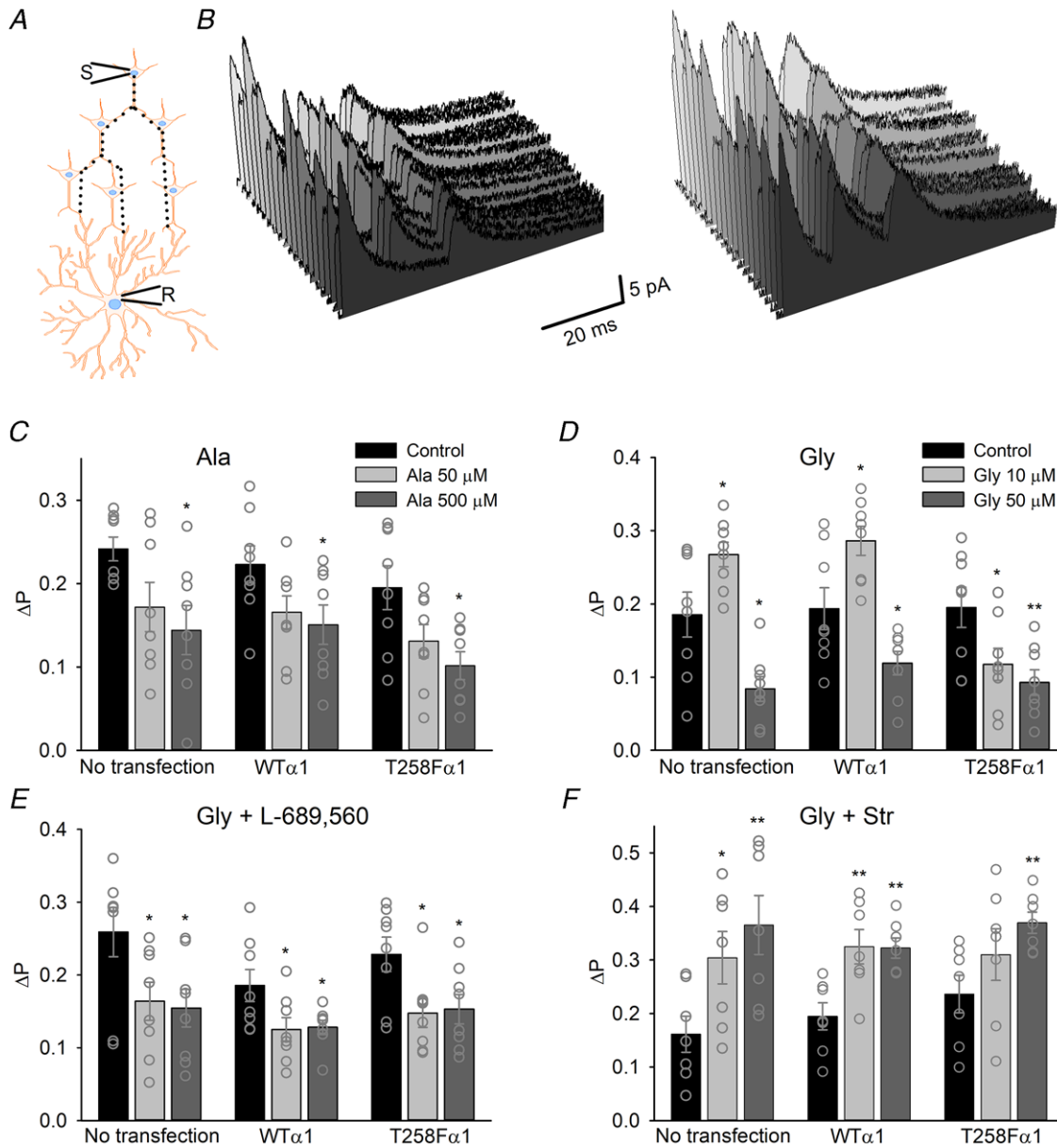
Figure 8. GlyRs modulate synaptic plasticity in a network of cultured CGCs
A, sketch depicting three hypothetical polysynaptic pathways (dotted lines) leading from stimulated neuron (S) to the recorded neuron (R) with different transmission delays, corresponding to the onset latencies of the three distinct eEPSC components. *B*, traces depict 20 consecutive eEPSCs (inward currents are shown upwards) recorded from a cultured neuron in response to stimulation of a nearby neuron before (left) and after repetitive paired-pulse stimulation (right). *C–F*, statistical summary of pathway remodelling induced by paired-pulse stimulation with modulatory impact of GlyR ligands. *C*, Ala applied. *D*, Gly applied; bar colour codes apply to *D–F*. *E*, Gly applied, NMDARs are blocked with 2 nM L-689,560. *F*, Gly applied, GlyRs are blocked with 1 μM strychnine. Asterisks denote significance of difference from control value. *$P < 0.05$, **$P < 0.01$, $n = 7$–8, Student's *t* test. [Colour figure can be viewed at wileyonlinelibrary.com]
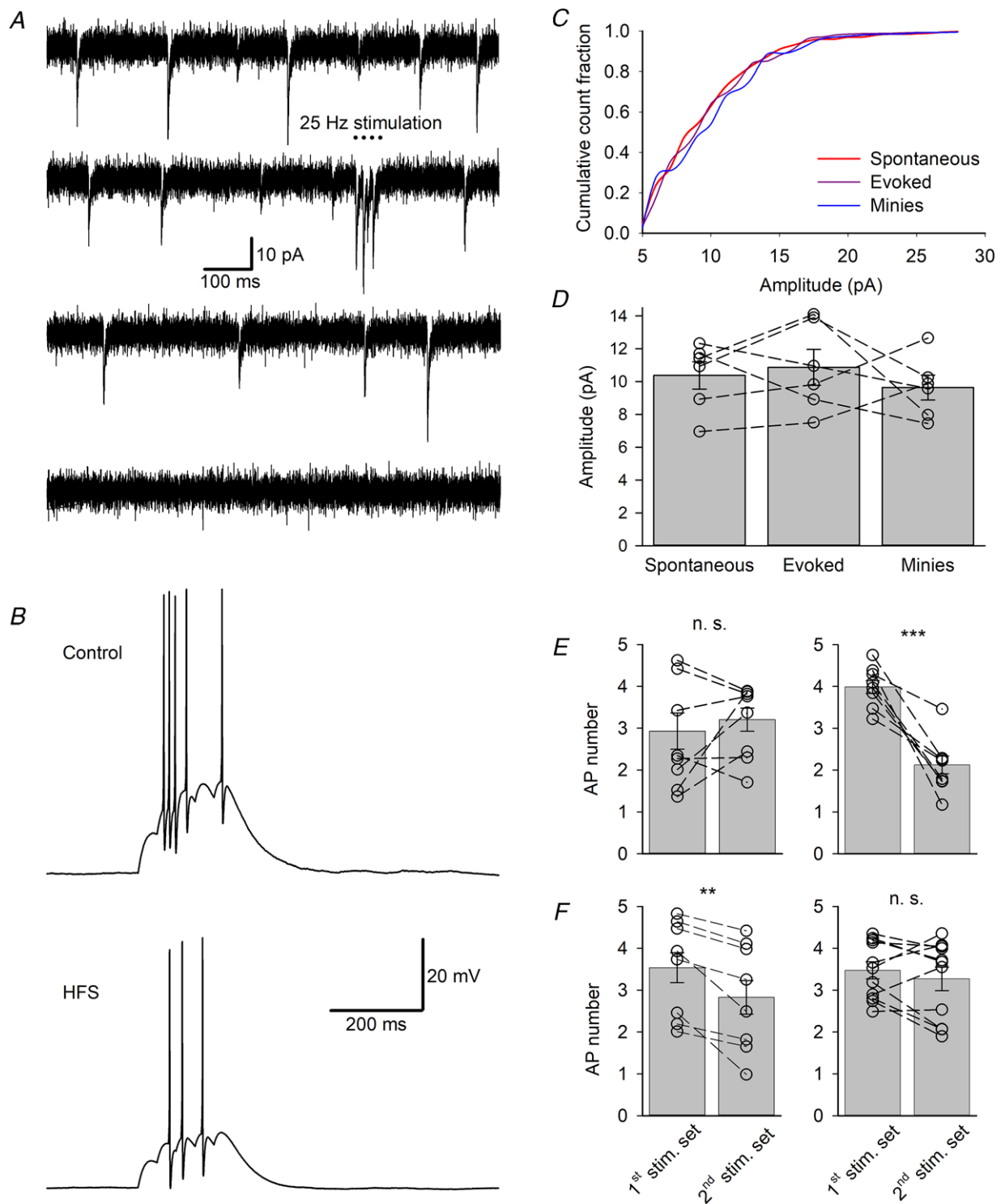
Figure 9. GlyRs modulate AP generation in CGCs of acute tissue

A, examples of glutamate-evoked excitatory responses in CGCs. From top to bottom, spontaneous activity; spontaneous activity and eEPSC burst evoked by 5 stimuli at 25 Hz delivered through single mossy fibre; mini-eEPSCs after TTX application; all activity suppressed by 50 μM NBQX application. *B*, example action potentials evoked by 5 stimuli at 25 Hz through single mossy fibre. Top, control. Bottom, after HFS. *C*, normalized cumulative amplitude histograms for spontaneous eEPSCs, eEPSCs evoked by 25 Hz stimulation, and mini-eEPSCs, 1 pA bin. *D*, statistical summary for *A*. Average amplitudes of spontaneous eEPSCs, eEPSCs evoked by 25 Hz stimulation, and mini-eEPSCs, *n* = 6 cells; 25 Hz stimulation: 10–15 episodes 30 s apart in each cell. *E* and *F*, statistical summary for *B*. Shift in average number of APs generated by 25 Hz stimulation series: 1st stimulation set of 4

number of APs per stimulation group: 2.12 ± 0.21 *vs.* 3.98 ± 0.16 in the first stimulation set, $P = 0.00011$, $n = 9$, Student's paired *t* test. To advance on this and to investigate whether cerebellar tissue can release an amount of Gly sufficient to modulate AP generation, we repeated the experiment with HFS (8 bursts of 10 impulses at 100 Hz, delivered to mossy fibres by tungsten bipolar electrode) after the first stimulation set. In this case AP number per five-stimuli group in the second stimulation set was significantly reduced: 2.83 ± 0.4 *vs.* 3.53 ± 0.36 in the first set, $P = 0.0014$, $n = 9$, Student's paired *t* test. To test whether this effect was indeed delivered by GlyRs, we repeated the HFS experiment adding 1 μM strychnine after the first stimulation set. Strychnine made difference in AP number between the first and second stimulation sets non-significant, thus confirming GlyR involvement: 3.47 ± 0.21 *vs.* 3.27 ± 0.28, $P = 0.31$, $n = 11$, Student's paired *t* test.

Discussion

In this study as a first stage we clarified the functional effects of GlyR subunits. We found that the single-point T258F mutation of the $\alpha1$ subunit decreases EC_{50} of Gly and Ala (Fig. 1 and Tables 1 and 2) and slows the decay kinetics of the inhibitory response delivered via heteromeric receptors (Fig. 3). This proves that the T258F mutation increases GlyR affinity to agonists, which is in line with earlier observations (Shan *et al.* 2001). In addition, the augmented affinity outweighs the lower conductance of T258F GlyR (compared to the WT receptor) (Fig. 2). However, contrary to Shan *et al.* (2001), in our preparation WT heteromeric ($\alpha1\beta$) GlyRs displayed a significantly higher affinity to agonists than did WT homomeric $\alpha1$ GlyRs (Table 1). This resembles another study in which heteromeric GlyRs were shown to have significantly lower EC_{50} for Gly than did homomeric receptors (Mohammadi *et al.* 2003). Overall, these facts suggest prudence when predicting GlyR effects on the basis of the receptor subunit composition. Nonetheless, experiments on HEK-293 cells have clearly shown that the introduction of the T258F$\alpha1$ subunit increases affinity to agonists in both hetero- and homomeric GlyRs, i.e. confirmed a gain-of-function status of the T258F mutation.

Factors determining the existence of multiple conductance states in GlyRs and mechanisms of their implementation are the topic of long-lasting discussions.

The most obvious explanation is that GlyRs can open to various conductance states in response to different ligation levels: from one to five agonist molecules bound to the functional receptor (Beato *et al.* 2004), as was demonstrated for the closely related $GABA_AR$ (Birnir *et al.* 2001). This, however, was disproved by observations that the ratio of GlyR openings to different conductance levels is independent of the agonist concentration (Twyman & Macdonald, 1991; Beato *et al.* 2002). Number and conductivity of GlyR conductance levels were repeatedly shown to be regulated by the receptor subunit composition (Rajendra *et al.* 1997), where presence of the β subunit eliminates high-conductance levels (Bormann *et al.* 1993). Hence, another possibility to obtain different conductance levels in the same patch recording is the presence of GlyRs of different subunit composition in a given membrane patch. This option, however, looks quite unlikely due to observations of openings to distinct conductance levels within the same burst (Beato *et al.* 2002). The presence of different conductance levels in recordings from outside-out patches (as in Fig. 6), where all cytoplasmic signalling chains are surely destroyed (Hamill *et al.* 1983; Takahashi *et al.* 1992), also questions modulation by intracellular factors as the only mechanism generating different GlyR conductance states. Therefore, the available experimental facts about propagation of GlyR conductance levels suggest multiple mechanisms of their modulation. In this context, the lower number of conductance levels in outside-out patches than in nucleated patches observed in our study (two *vs.* three) may be a result of removal of cytoplasmic factor(s) delivering a partial upregulatory effect in living cells.

Residue position 258 in all types of GlyR subunits is localized within the M2 domain which lines the receptor ion channel pore, making GlyR electrical conductance highly sensitive to mutations in this domain (Keramidas *et al.* 2000, 2002). Therefore, it is not surprising that the T258F mutation, i.e. replacement of a small, polar and hydrophilic threonine residue with a large, non-polar and hydrophobic phenylalanine, exerts a significant down-regulatory effect on GlyR electrical conductance, possibly by obstructing Cl^- ion passage.

The issue to be clarified for work on GlyRs expressed in acute tissue is indeed their actual subunit composition. *In situ* hybridization experiments on mRNA encoding various GlyR subunits have shown that the expression level of the $\alpha1$ subunit increases, and that of the $\alpha2$ subunit decreases rapidly in postnatal (after P0) tissue of spinal

groups of 5 stimuli at 25 Hz with 30 s intervals, then 5 min interval, and 2nd stimulation set similar to the first. *E*, no HFS. Left, control. Right, Gly 50 μM added after 1st stimulation set. *F*, HFS after the 1st stimulation set. Left, control. Right, strychnine 1 μM added after the 1st stimulation set. Bar titles and vertical axis titles apply to all bar charts in *E* and *F*. Asterisks denote significance of difference between average number of APs in 1st and 2nd stimulation set; **$P < 0.01$, *** $P < 0.001$, $n = 9$–11, Student's paired *t* test. [Colour figure can be viewed at wileyonlinelibrary.com]

cord (Watanabe & Akagi, 1995). Similar experiments conducted by different research groups on the CGC layer of adult rodents generated various results: a strong signal for α1 mRNA with somatic localization (Racca *et al.* 1998), a weak signal for α1 mRNA (Fujita *et al.* 1991), or no detection for both α1 and α2 subunit mRNA (Sato *et al.* 1992). We thus tried to assess the input of α1-containing GlyRs into the overall GlyR signal with an alternative approach. In line with an earlier study (Li & Slaughter, 2007), we found that 1 mM BIC, applied with 60 μM Gly, fully suppresses opening of α2-containing GlyRs expressed in HEK cells, but has much lower impact when α1-containing GlyRs were expressed. Then, being applied on GlyRs from acute cerebellar tissue, BIC approximately halved GlyR-mediated current, thus confirming a significant role of α1-GlyRs in living CGCs (Fig. 4*C* and *E*).

In our experiments on HEK cells, cultured CGCs and CGCs from acute tissue, we have not observed a significant difference between heteromeric GlyRs in terms of pharmacological properties (EC_{50}, IC_{50}, Hill's coefficients) and ion channel conductance, along with similarities in percentage of overall charge transfer through given conductance state (see Tables 1–4). The impact of the T258F mutation on GlyR response decay kinetics in transfected CGCs resembles that obtained in HEK cells (Fig. 3). Moreover, PTX displayed a negligible effect on heteromeric GlyRs expressed in cultured cells and on GlyRs in membrane patches excised from CGCs of cerebellar slices (Fig. 4), thus confirming the long-established finding of PTX antagonism at WTα1 homomeric, but not T258Fα1 homomeric or any type of heteromeric GlyRs (Pribilla *et al.* 1992; Shan *et al.* 2001). These observations suggest three main conclusions. First, physiological and pharmacological properties of GlyRs in living tissue and of heteromeric WT GlyRs expressed in different types of cultured cells are similar. Second, most GlyRs in native CGCs of 25- to 30-day-old mice are of heteromeric composition. Third, native expression of β GlyR subunit in CGCs is high enough to make most of the GlyRs heteromeric when the cell is transfected with an additional amount of α-subunit DNA; this is in accord with earlier data on much higher expression of the β GlyR subunit than the α subunit in postnatal CGCs (van den Pol & Gorcs, 1988; Fujita *et al.* 1991).

The data on GlyR presence at CGC somata at different ages are to some extent contradictory. Wall & Usowicz (1997) reported the presence of GlyR-mediated currents for P12 but not for P40 animals; on the contrary, Sassoè-Pognetto *et al.* (2000) found GlyR-specific immunostaining in CGCs of adult rats. A plausible explanation of such an apparent discrepancy is that GlyR number at the CGC soma decreases with age, making, at some stage, GlyR-mediated tonic current undetectable under normal conditions. Under these conditions GlyRs,

however, can still be detected with immunostaining and may deliver a significant amount of tonic current after HFS, which provokes neurotransmitter spillover. Therefore, to test this hypothesis and clarify a functional role of GlyRs in CGC layer, we next studied GlyR signalling in acute cerebellar tissue.

The absence of spontaneous postsynaptic currents after the isolation of a GlyR-mediated response in our whole-cell recordings (Fig. 5*A*) confirms earlier reports about CGCs being deprived of functional synaptic GlyRs, but carrying them at extrasynaptic membrane (Huck & Lux, 1987; Kaneda *et al.* 1995; Virginio & Cherubini, 1997).

There are several possible explanations of lower amounts of GlyR-transferred current observed in CGCs than in HEK cells (see Figs 1, 4 and 5). First, size and surface area of HEK cells are substantially larger than those of CGCs: this is illustrated by cell images (Fig. 3*G*) and by data on membrane capacitance (11.16 ± 0.2 pS for HEKs *vs.* 2.903 ± 0.11 pS for CGCs; see Methods). Second, the expression level and, as a consequence, density of GlyRs at cell somata could be different for HEK cells and CGCs. This was confirmed by experiments finding that Gly application at membrane patches excised from HEK cells elicited macroscopic responses (Fig. 3*A* and *C*), whereas the majority of outside-out patches obtained from CGCs after application of Gly displayed single-channel openings; to generate macroscopic GlyR responses in patches from CGCs, the use of nucleated patches with much larger surface area was necessary (Fig. 3*E*). Third, as CGCs, in contrast to HEK cells, have a branched shape with several neurites (Fig. 3*G*), and GlyR density at dendrites increases with distance from the cell soma (Lorenzo *et al.* 2007), in whole-cell recordings (as in Figs 1*A*–*D* and 5) the decrease of response amplitude due to a space-clamp effect should be much stronger in CGCs than in HEK cells.

GlyR-mediated tonic inhibition was shown to shape neuronal network behaviour in acute neural tissue (Flint *et al.* 1998; Zhang *et al.* 2008) but, to the best of our knowledge, not in the cerebellum; in our work, we could not register a significant GlyR input into tonic current under normal conditions (Fig. 5*A*). A plausible explanation is a low concentration of GlyR agonists in cerebellar extracellular space under stable conditions. Despite the fact that the release of Gly and Ala was repeatedly detected in native cerebellum (Koga *et al.* 2002; Billups & Attwell, 2003) and, in particular, in cerebellar vermis (Flint *et al.* 1981), their level in the extracellular space were reported in a range of tens of micromoles (Tossman *et al.* 1986; Takagi *et al.* 1993; Westergren *et al.* 1994; Oda *et al.* 2007), which is just above the detectable level of Gly for WT receptors found in our work, and far below this level for Ala (see Fig. 1 and Table 1). Taken together with relatively low levels of expression of GlyRs in CGCs, when compared to neighbouring interneurons of cerebellar molecular layer and Purkinje cells (van den Pol

& Gorcs, 1988; Racca *et al.* 1998; Sassoè-Pognetto *et al.* 2000), this may result in a very small amount of tonic current, undetectable with electrophysiological methods. However, HFS generated a highly significant inhibitory charge transfer via GlyRs; similar results obtained in experiments with elevated Ca^{2+} concentration support a hypothesis of upregulation of neurotransmitter release as a mechanism of tonic current generation by HFS (Fig. 5*D*). These observations also imply that the extrasynaptic GlyRs of CGCs play their functional role not on a continuous basis, but when the CGC layer starts receiving a high amount of excitatory inputs.

Our experimental findings on the generation of an EPSP series confirmed that GlyR input into electrical conductance exerts a substantial effect on inter-neuronal crosstalk (Fig. 7). The amount of inhibitory current transferred via GlyRs is sufficient for the control of AP generation, thus resembling the functions of tonically active GlyRs in the spinal cord (Takazawa & MacDermott, 2010).

In our subsequent experiments on the remodelling of signalling pathways, we demonstrated that the activation of GlyRs by a series of paired stimuli exerts a significant impact on the variability of synaptic transmission and synaptic strength (ΔP) – Fig. 8. Varying Gly concentrations caused an inverse change of ΔP: an increase for low concentration and a decrease for high (Fig. 8*D*). Since such a change of ΔP was not observed in the experiment involving Ala, when Gly was added together with L-689,560 and when GlyRs were blocked with Str (Fig. 8*C*, *E* and *F*), we concluded that this biphasic effect requires simultaneous presence of active GlyRs and NMDARs. Therefore, we formulated a hypothesis regarding the functional role of GlyR signalling in CGCs as follows. Gly is a co-agonist that is critical for NMDAR functioning, and the elevation of incoming signalling intensity enhances Gly concentration in the CGC layer (Billups & Attwell, 2003), thus ensuring NMDAR activation and AP generation. However, a further increment of signalling strength activates extrasynaptic GlyRs due to the amplification of the Gly concentration. This, in turn, suppresses AP firing in CGCs and therefore discontinues (or at least limits) outgoing signalling. This hypothesis provides a plausible explanation for GlyRs' relative scarcity (Sassoè-Pognetto *et al.* 2000) and their exclusive extrasynaptic localization (Kaneda *et al.* 1995): these are the obligatory characteristics that ensure the biphasic modulation of the cell signalling output, amplifying the excitatory input at low intensity, but triggering a 'safety catch' which limits further excitation when input signalling rises to a certain critical level. In our experiments, T258F GlyRs, having a higher affinity to Gly, will inhibit CGC firing with a lower concentration of neurotransmitter spillover, which is equivalent to much weaker excitatory input.

To the best of our knowledge, there are no reports about significant Gly release (and, more importantly, spillover) in CGC synapses in response to increased excitatory input; this is in accord with the fact of the absence of GlyRs in CGC synapses (Kaneda *et al.* 1995). Therefore, since CGCs make up >97% of the neuronal population of the granule cell layer (Herndon, 1964; Palay & Chan-Palay, 2012), the question about a particular mechanism of the excitation-induced Gly concentration increase in the CGC layer becomes critical in a context of our hypothesis regarding Gly-based biphasic modulation of CGC activity. The possible source of Gly concentration increase is the Bergmann glia, which are abundant in the CGC layer (Herndon, 1964; Southam *et al.* 1992) and release significant amounts of Gly in response to cell membrane depolarization (Huang *et al.* 2004). Such a depolarization might be due to glutamate spillover from neuronal synapses upon overexcitation, and subsequent activation of NMDA and AMPA receptors at Bergmann glial cells, which was shown to induce powerful cation inflow (Müller *et al.* 1993; Dzubay & Jahr, 1999). Therefore, the critical level of excitatory input which switches Gly-mediated inhibition in CGC layer might be to a large extent determined by the distribution of the glial Gly transporter GLYT1 (Zafra *et al.* 1995), its activity, and its sensitivity to cell membrane depolarization (Huang *et al.* 2004).

Another important question about Gly-mediated inhibition of CGC activity is with regard to its inter-action and/or mutual influence with other biphasic modulatory systems in the CGC layer, such as the glutamate–nitric oxide (NO)–cGMP pathway. In this pathway NO was shown to be a retrograde neuro-transmitter which determines presynaptic ion currents, neural network excitability and long-term potentiation. In turn, NO pathway blockers inhibit neural cell excitation and long-term potentiation (D'Angelo *et al.* 2005). It was reported earlier that when released from cerebellar neurons, NO activates soluble guanylate cyclase, thus increasing the amount of cGMP in Bergmann glia (Southam *et al.* 1992) and in this way reducing Gly release (Hernandes & Troncone, 2009). This suggests the phenomenon of Gly-mediated biphasic regulation of CGC signalling to be an integral and tightly inter-connected part of regulatory mechanisms (such as the NO–cGMP pathway) that modulate cerebellar neural activity.

Our next experiment on AP generation in response to sensory-like excitatory signalling, which resembles the effect of stimulation of the rodent's whisker (Chadderton *et al.* 2004), proved a significant input of GlyRs into the CGC excitation machinery in living cerebellar tissue, and provided further support for the hypothesis regarding the GlyRs' functional role. We have shown that intensive excitatory signalling activates a GlyR-mediated 'safety

catch' which prevents over-excitation of CGCs in response to sensory inputs (Fig. 9).

An earlier study has shown that CGCs, generating bursts of APs of limited length in response to clustered sensory-evoked signals from mossy fibres, produce patterns of activity which provide a physiological mechanism for the model of the CGC layer as a storage of sensory representations (Chadderton *et al.* 2004). Within this model the strictly limited intensity of outgoing signalling increases the CGC layer's capacity to act as an information store (Marr, 1969; Albus, 1971). This suggests a GlyR-generated 'safety catch' as the element controlling a key function of the cerebellar granule layer. In turn, the GlyRs which underwent a gain-of-function mutation, due to their higher affinity, might break the cerebellar mechanism of sensory representation formation, storage and translation into motor outputs.

Classical GlyR mutations which lead to hyperekplexia development are the loss-of-function mutations that reduce Cl⁻ inhibitory current (Harvey *et al.* 2008); it is widely accepted that such a deficiency of inhibition provokes a massive haphazard motor activity in response to an unexpected and/or uncommon sensory stimulus (Matsumoto *et al.* 1992). On the other hand, GlyR gain-of-function mutations (with effects similar to T258F) were also shown to induce hyperekplexia (Chung *et al.* 2010; Bode *et al.* 2013). It seems, then, paradoxical that mutations of opposite effect generate similar disease manifestations and full clinical syndrome. To date, the only proposed explanation is that enhanced spontaneous GlyR activity due to gain-of-function mutation during nervous system development prevents formation of glycinergic synapses and thus induces shortage of inhibitory signalling in adult brain (Zhang *et al.* 2016). This, however, is unlikely the case for CGCs in cerebellar vermis, which are deprived of glycinergic synapses under healthy conditions. Nevertheless, it was repeatedly demonstrated that hyperekplexia is associated with functional deficits in cerebellar vermis (Leaton & Supple, 1986; Lopiano *et al.* 1990; Goraya *et al.* 2002). Thus one more possible explanation of cerebellar hyperekplexia mechanisms is as follows. The gain-of-function mutation, due to over-amplification of the 'safety catch', disrupts the process of induction of standard activity patterns, stored in the CGC layer (Chadderton *et al.* 2004), in response to sensory inputs (as was shown in our experiment with sensory input-mimicking stimulation; Fig. 9), and thus leads to chaotic movement reactions. Alternatively, one should assume that CGCs, which are the most numerous neurons in the brain and make up ∼90% of neurons in the cerebellum, have, nevertheless, no connection to cerebellum-associated hyperekplexia effects.

Our data demonstrate that fluctuations of GlyR-delivered tonic inhibition due to the T258F mutation make a significant impact on single-receptor, single-cell and neuronal network functioning in the CGC layer. The fundamental question is, however, whether modulation of GlyR inhibitory tone can lead to abnormalities at the level of the whole organism. The impact on single-cell signalling due to genetic deletion of α6 and δ subunits of the GABA_AR which deprived CGCs of the major amount of tonic inhibition was shown to be compensated by alternative signalling mechanisms (Brickley *et al.* 2001). In line with this, genetic silencing of expression of the α1 GABA_AR subunit can lead to the loss of ∼60% of functional GABA_ARs in the brain; but, nevertheless, the connected effects on animal phenotype and behaviour can be successfully compensated (Reynolds *et al.* 2003). These observations suggest behavioural studies with animal model(s) with CGC-specific GlyR mutations as the next step in clarification of cerebellar mechanisms of hyperekplexia.

References

Albus JS (1971). A theory of cerebellar function. *Math Biosci* **10**, 25–61.

Avila G, Sandoval A & Felix R (2004). Intramembrane charge movement associated with endogenous K⁺ channel activity in HEK-293 Cells. *Cell Mol Neurobiol* **24**, 317–330.

Beato M, Groot-Kormelink PJ, Colquhoun D & Sivilotti LG (2002). Openings of the rat recombinant α1 homomeric glycine receptor as a function of the number of agonist molecules bound. *J Gen Physiol* **119**, 443–466.

Beato M, Groot-Kormelink PJ, Colquhoun D & Sivilotti LG (2004). The activation mechanism of α1 homomeric glycine receptors. *J Neurosci* **24**, 895–906.

Bennett MR & Kearns JL (2000). Statistics of transmitter release at nerve terminals. *Prog Neurobiol* **60**, 545–606.

Bi G & Poo M (1999). Distributed synaptic modification in neural networks induced by patterned stimulation. *Nature* **401**, 792–796.

Billups D & Attwell D (2003). Active release of glycine or D-serine saturates the glycine site of NMDA receptors at the cerebellar mossy fibre to granule cell synapse. *Eur J Neurosci* **18**, 2975–2980.

Birnir B, Eghbali M, Cox GB & Gage PW (2001). GABA concentration sets the conductance of delayed GABA_A channels in outside-out patches from rat hippocampal neurons. *J Membr Biol* **181**, 171–183.

Blednov YA, Benavidez JM, Homanics GE & Harris RA (2012). Behavioral characterization of knockin mice with mutations M287L and Q266I in the glycine receptor alpha1 subunit. *J Pharmacol Exp Ther* **340**, 317–329.

Bode A, Wood SE, Mullins JG, Keramidas A, Cushion TD, Thomas RH, Pickrell WO, Drew CJ, Masri A, Jones EA, Vassallo G, Born AP, Alehan F, Aharoni S, Bannasch G, Bartsch M, Kara B, Krause A, Karam EG, Matta S, Jain V, Mandel H, Freilinger M, Graham GE, Hobson E, Chatfield S, Vincent-Delorme C, Rahme JE, Afawi Z, Berkovic SF, Howell OW, Vanbellinghen JF, Rees MI, Chung SK & Lynch JW (2013). New hyperekplexia mutations provide insight

into glycine receptor assembly, trafficking, and activation mechanisms. *J Biol Chem* **288**, 33745–33759.

Bormann J, Rundstrom N, Betz H & Langosch D (1993). Residues within transmembrane segment M2 determine chloride conductance of glycine receptor homo- and hetero-oligomers. *EMBO J* **12**, 3729–3737.

Brickley SG, Revilla V, Cull-Candy SG, Wisden W & Farrant M (2001). Adaptive regulation of neuronal excitability by a voltage-independent potassium conductance. *Nature* **409**, 88–92.

Chadderton P, Margrie TW & Häusser M (2004). Integration of quanta in cerebellar granule cells during sensory processing. *Nature* **428**, 856–860.

Chen C & Okayama H (1987). High-efficiency transformation of mammalian cells by plasmid DNA. *Mol Cell Biol* **7**, 2745–2752.

Chung SK, Vanbellinghen JF, Mullins JG, Robinson A, Hantke J, Hammond CL, Gilbert DF, Freilinger M, Ryan M, Kruer MC, Masri A, Gurses C, Ferrie C, Harvey K, Shiang R, Christodoulou J, Andermann F, Andermann E, Thomas RH, Harvey RJ, Lynch JW & Rees MI (2010). Pathophysiological mechanisms of dominant and recessive GLRA1 mutations in hyperekplexia. *J Neurosci* **30**, 9612–9620.

Clarkson AN, Huang BS, MacIsaac SE, Mody I & Carmichael ST (2010). Reducing excessive GABA-mediated tonic inhibition promotes functional recovery after stroke. *Nature* **468**, 305–309.

Corda MG, Orlandi M, Lecca D, Carboni G, Frau V & Giorgi O (1991). Pentylenetetrazol-induced kindling in rats: effect of GABA function inhibitors. *Pharmacol Biochem Behav* **40**, 329–333.

D'Angelo E, De Filippi G, Rossi P & Taglietti V (1995). Synaptic excitation of individual rat cerebellar granule cells in situ: evidence for the role of NMDA receptors. *J Physiol* **484**, 397–413.

D'Angelo E, Rossi P, Armano S & Taglietti V (1999). Evidence for NMDA and mGlu receptor-dependent long-term potentiation of mossy fiber-granule cell transmission in rat cerebellum. *J Neurophysiol* **81**, 277–287.

D'Angelo E, Rossi P, Gall D, Prestori F, Nieus T, Maffei A & Sola E (2005). Long-term potentiation of synaptic transmission at the mossy fiber-granule cell relay of cerebellum. *Prog Brain Res* **148**, 69–80.

Dzubay JA & Jahr CE (1999). The concentration of synaptically released glutamate outside of the climbing fiber-Purkinje cell synaptic cleft. *J Neurosci* **19**, 5265–5274.

Eulenburg V & Gomeza J (2010). Neurotransmitter transporters expressed in glial cells as regulators of synapse function. *Brain Res Rev* **63**, 103–112.

Farrant M & Nusser Z (2005). Variations on an inhibitory theme: phasic and tonic activation of GABA$_A$ receptors. *Nat Rev Neurosci* **6**, 215–229.

Fischmeister R & Hartzell HC (2005). Volume sensitivity of the bestrophin family of chloride channels. *J Physiol* **562**, 477–491.

Flint AC, Liu X & Kriegstein AR (1998). Nonsynaptic glycine receptor activation during early neocortical development. *Neuron* **20**, 43–53.

Flint RS, Rea MA & McBride WJ (1981). In vitro release of endogenous amino acids from granule cell-, stellate cell-, and climbing fiber-deficient cerebella. *J Neurochem* **37**, 1425–1430.

Fujita M, Sato K, Sato M, Inoue T, Kozuka T & Tohyama M (1991). Regional distribution of the cells expressing glycine receptor β subunit mRNA in the rat brain. *Brain Res* **560**, 23–37.

Garthwaite J & Batchelor AM (1996). A biplanar slice preparation for studying cerebellar synaptic transmission. *J Neurosci Methods* **64**, 189–197.

Goraya JS, Shah D & Poddar B (2002). Hyperekplexia in a girl with posterior fossa malformations. *J Child Neurol* **17**, 147–149.

Grimwood S, Moseley AM, Carling RW, Leeson PD & Foster AC (1992). Characterization of the binding of [^{3}H]L-689,560, an antagonist for the glycine site on the N-methyl-D-aspartate receptor, to rat brain membranes. *Mol Pharmacol* **41**, 923–930.

Hamann M, Rossi DJ & Attwell D (2002). Tonic and spillover inhibition of granule cells control information flow through cerebellar cortex. *Neuron* **33**, 625–633.

Hamill OP, Bormann J & Sakmann B (1983). Activation of multiple-conductance state chloride channels in spinal neurones by glycine and GABA. *Nature* **305**, 805–808.

Harvey RJ, Topf M, Harvey K & Rees MI (2008). The genetics of hyperekplexia: more than startle! *Trends Genet* **24**, 439–447.

Hashimoto A, Oka T & Nishikawa T (1995). Extracellular concentration of endogenous free D-serine in the rat brain as revealed by in vivo microdialysis. *Neuroscience* **66**, 635–643.

Hernandes MS & Troncone LRP (2009). Glycine as a neurotransmitter in the forebrain: a short review. *J Neural Transm* **116**, 1551–1560.

Herndon RM (1964). The fine structure of the rat cerebellum. II. The stellate neurons, granule cells, and glia. *J Cell Biol* **23**, 277–293.

Hevers W & Lüddens H (2002). Pharmacological heterogeneity of γ-aminobutyric acid receptors during development suggests distinct classes of rat cerebellar granule cells in situ. *Neuropharmacology* **42**, 34–47.

Huang H, Barakat L, Wang D & Bordey A (2004). Bergmann glial GlyT1 mediates glycine uptake and release in mouse cerebellar slices. *J Physiol* **560**, 721–736.

Huck S & Lux HD (1987). Patch-clamp study of ion channels activated by GABA and glycine in cultured cerebellar neurons of the mouse. *Neurosci Lett* **79**, 103–107.

Kaneda M, Farrant M & Cull-Candy SG (1995). Whole-cell and single-channel currents activated by GABA and glycine in granule cells of the rat cerebellum. *J Physiol* **485**, 419–435.

Keramidas A, Moorhouse AJ, French CR, Schofield PR & Barry PH (2000). M2 pore mutations convert the glycine receptor channel from being anion- to cation-selective. *Biophys J* **79**, 247–259.

Keramidas A, Moorhouse AJ, Pierce KD, Schofield PR & Barry PH (2002). Cation-selective mutations in the M2 domain of the inhibitory glycine receptor channel reveal

determinants of ion-charge selectivity. *J Gen Physiol* **119**, 393–410.

Koga T, Kozaki S & Takahashi M (2002). Exocytotic release of alanine from cultured cerebellar neurons. *Brain Res* **952**, 282–289.

Langosch D, Thomas L & Betz H (1988). Conserved quaternary structure of ligand-gated ion channels: the postsynaptic glycine receptor is a pentamer. *Proc Natl Acad Sci U S A* **85**, 7394–7398.

Leaton R & Supple W (1986). Cerebellar vermis: essential for long-term habituation of the acoustic startle response. *Science* **232**, 513–515.

Li P & Slaughter M (2007). Glycine receptor subunit composition alters the action of GABA antagonists. *Vis Neurosci* **24**, 513–521.

Lopiano L, de'Sperati C & Montarolo PG (1990). Long-term habituation of the acoustic startle response: Role of the cerebellar vermis. *Neuroscience* **35**, 79–84.

Lorenzo L-E, Russier M, Barbe A, Fritschy J-M & Bras H (2007). Differential organization of γ-aminobutyric acid type A and glycine receptors in the somatic and dendritic compartments of rat abducens motoneurons. *J Comp Neurol* **504**, 112–126.

Losi G, Prybylowski K, Fu Z, Luo JH & Vicini S (2002). Silent synapses in developing cerebellar granule neurons. *J Neurophysiol* **87**, 1263–1270.

Lynch JW (2009). Native glycine receptor subtypes and their physiological roles. *Neuropharmacology* **56**, 303–309.

Mann EO & Mody I (2009). Control of hippocampal gamma oscillation frequency by tonic inhibition and excitation of interneurons. *Nat Neurosci* **13**, 205–212.

Marr D (1969). A theory of cerebellar cortex. *J Physiol* **202**, 437–470.

Matsui T, Sekiguchi M, Hashimoto A, Tomita U, Nishikawa T & Wada K (1995). Functional comparison of D-serine and glycine in rodents: the effect on cloned NMDA receptors and the extracellular concentration. *J Neurochem* **65**, 454–458.

Matsumoto J, Fuh P, Nigro M & Hallett M (1992). Physiological abnormalities in hereditary hyperekplexia. *Ann Neurol* **32**, 41–50.

Mohammadi B, Krampfl K, Cetinkaya C, Moschref H, Grosskreutz J, Dengler R & Bufler J (2003). Kinetic analysis of recombinant mammalian α_1 and $\alpha_1\beta$ glycine receptor channels. *Eur Biophys J* **32**, 529–536.

Mori M, Gähwiler BH & Gerber U (2002). β-Alanine and taurine as endogenous agonists at glycine receptors in rat hippocampus in vitro. *J Physiol* **539**, 191–200.

Mtchedlishvili Z & Kapur J (2006). High-affinity, slowly desensitizing GABA$_A$ receptors mediate tonic inhibition in hippocampal dentate granule cells. *Mol Pharmacol* **69**, 564–575.

Müller T, Grosche J, Ohlemeyer C & Kettenmann H (1993). NMDA-activated currents in Bergmann glial cells. *Neuroreport* **4**, 671–674.

Oda M, Kure S, Sugawara T, Yamaguchi S, Kojima K, Shinka T, Sato K, Narisawa A, Aoki Y, Matsubara Y, Omae T, Mizoi K & Kinouchi H (2007). Direct correlation between ischemic injury and extracellular glycine concentration in mice with genetically altered activities of the glycine cleavage multienzyme system. *Stroke* **38**, 2157–2164.

Palay SL & Chan-Palay V (2012). *Cerebellar Cortex: Cytology and Organization.* Springer-Verlag, Berlin Heidelberg.

Pan ZH & Slaughter MM (1995). Comparison of the actions of glycine and related amino acids on isolated third order neurons from the tiger salamander retina. *Neuroscience* **64**, 153–164.

Pribilla I, Takagi T, Langosch D, Bormann J & Betz H (1992). The atypical M2 segment of the β subunit confers picrotoxinin resistance to inhibitory glycine receptor channels. *EMBO J* **11**, 4305–4311.

Racca C, Gardiol A & Triller A (1998). Cell-specific dendritic localization of glycine receptor α subunit messenger RNAs. *Neuroscience* **84**, 997–1012.

Rajendra S, Lynch JW & Schofield PR (1997). The glycine receptor. *Pharmacol Ther* **73**, 121–146.

Reynolds DS, O'Meara GF, Newman RJ, Bromidge FA, Atack JR, Whiting PJ, Rosahl TW & Dawson GR (2003). GABA$_A$ α1 subunit knock-out mice do not show a hyperlocomotor response following amphetamine or cocaine treatment. *Neuropharmacology* **44**, 190–198.

Rossi DJ, Hamann M & Attwell D (2003). Multiple modes of GABAergic inhibition of rat cerebellar granule cells. *J Physiol* **548**, 97–110.

Salling MC & Harrison NL (2014). Strychnine-sensitive glycine receptors on pyramidal neurons in layers II/III of the mouse prefrontal cortex are tonically activated. *J Neurophysiol* **112**, 1169–1178.

Saransaari P & Oja SS (1993). Uptake and release of β-alanine in cerebellar granule cells in primary culture: Regulation of release by glutamatergic and GABAergic receptors. *Neuroscience* **53**, 475–481.

Sassoè-Pognetto M, Panzanelli P, Sieghart W & Fritschy JM (2000). Colocalization of multiple GABA$_A$ receptor subtypes with gephyrin at postsynaptic sites. *J Comp Neurol* **420**, 481–498.

Sato K, Kiyama H & Tohyama M (1992). Regional distribution of cells expressing glycine receptor α2 subunit mRNA in the rat brain. *Brain Res* **590**, 95–108.

Shan Q, Haddrill JL & Lynch JW (2001). A single β subunit M2 domain residue controls the picrotoxin sensitivity of alphabeta heteromeric glycine receptor chloride channels. *J Neurochem* **76**, 1109–1120.

Southam E, Morris R & Garthwaite J (1992). Sources and targets of nitric oxide in rat cerebellum. *Neurosci Lett* **137**, 241–244.

Steinbach JH, Bracamontes J, Yu L, Zhang P & Covey DF (2000). Subunit-specific action of an anticonvulsant thiobutyrolactone on recombinant glycine receptors involves a residue in the M2 membrane-spanning region. *Mol Pharmacol* **58**, 11–17.

Sylantyev S & Rusakov DA (2013). Sub-millisecond ligand probing of cell receptors with multiple solution exchange. *Nat Protoc* **8**, 1299–1306.

Takagi K, Ginsberg MD, Globus MY, Dietrich WD, Martinez E, Kraydieh S & Busto R (1993). Changes in amino acid neurotransmitters and cerebral blood flow in the ischemic penumbral region following middle cerebral artery occlusion in the rat: correlation with histopathology. *J Cereb Blood Flow Metab* **13**, 575–585.

Takahashi T, Momiyama A, Hirai K, Hishinuma F & Akagi H (1992). Functional correlation of fetal and adult forms of glycine receptors with developmental changes in inhibitory synaptic receptor channels. *Neuron* **9**, 1155–1161.

Takazawa T & MacDermott AB (2010). Glycinergic and GABAergic tonic inhibition fine tune inhibitory control in regionally distinct subpopulations of dorsal horn neurons. *J Physiol* **588**, 2571–2587.

Tossman U, Jonsson G & Ungerstedt U (1986). Regional distribution and extracellular levels of amino acids in rat central nervous system. *Acta Physiol Scand* **127**, 533–545.

Traynelis SF & Jaramillo F (1998). Getting the most out of noise in the central nervous system. *Trends Neurosci* **21**, 137–145.

Twyman RE & Macdonald RL (1991). Kinetic properties of the glycine receptor main- and sub-conductance states of mouse spinal cord neurones in culture. *J Physiol* **435**, 303–331.

van den Pol AN & Gorcs T (1988). Glycine and glycine receptor immunoreactivity in brain and spinal cord. *J Neurosci* **8**, 472–492.

Virginio C & Cherubini E (1997). Glycine-activated whole cell and single channel currents in rat cerebellar granule cells in culture. *Dev Brain Res* **98**, 30–40.

Wall MJ & Usowicz MM (1997). Development of action potential-dependent and independent spontaneous GABA$_A$ receptor-mediated currents in granule cells of postnatal rat cerebellum. *Eur J Neurosci* **9**, 533–548.

Wang P & Slaughter MM (2005). Effects of GABA receptor antagonists on retinal glycine receptors and on homomeric glycine receptor alpha subunits. *J Neurophysiol* **93**, 3120–3126.

Wang X, Veruki ML, Bukoreshtliev NV, Hartveit E & Gerdes HH (2010). Animal cells connected by nanotubes can be electrically coupled through interposed gap-junction channels. *Proc Natl Acad Sci U S A* **107**, 17194–17199.

Watanabe E & Akagi H (1995). Distribution patterns of mRNAs encoding glycine receptor channels in the developing rat spinal cord. *Neurosci Res* **23**, 377–382.

Westergren I, Nystrom B, Hamberger A, Nordborg C & Johansson BB (1994). Concentrations of amino acids in extracellular fluid after opening of the blood-brain barrier by intracarotid infusion of protamine sulfate. *J Neurochem* **62**, 159–165.

Xu T-L & Gong N (2010). Glycine and glycine receptor signaling in hippocampal neurons: Diversity, function and regulation. *Prog Neurobiol* **91**, 349–361.

Zafra F, Gomeza J, Olivares L, Aragón C & Giménez C (1995). Regional distribution and developmental variation of the glycine transporters GLYT1 and GLYT2 in the rat CNS. *Eur J Neurosci* **7**, 1342–1352.

Zhang LH, Gong N, Fei D, Xu L & Xu TL (2008). Glycine uptake regulates hippocampal network activity via glycine receptor-mediated tonic inhibition. *Neuropsychopharmacology* **33**, 701–711.

Zhang Y, Bode A, Nguyen B, Keramidas A & Lynch JW (2016). Investigating the mechanism by which gain-of-function mutations to the alpha1 glycine receptor cause hyperekplexia. *J Biol Chem* **291**, 15332–15341.

Additional information

Competing interests

Authors declare that they have no conflict of interests.

Author contributions

C.ML. contributed to experimental work on cell cultures and edited the paper draft; J.C. performed experimental work and data analysis and produced research software; A-M.O. contributed to experimental work on cell cultures; S.S. performed experimental work, data analysis, and wrote the paper which was then critically revised by all co-authors. All authors have read and approved the final version of this manuscript and agree to be accountable for all aspects of the work in ensuring that questions related to the accuracy or integrity of any part of the work are appropriately investigated and resolved. All persons designated as authors qualify for authorship, and all those who qualify for authorship are listed.